Russian Chemical Reviews **82** (4) 303 – 332 (2013) © 2013 Russian Academy of Sciences and Turpion Ltd

DOI 10.1070/RC2013v082n04ABEH004322

New approaches to the development of hybrid nanocomposites: from structural materials to high-tech applications

V A Gerasin, E M Antipov, V V Karbushev, V G Kulichikhin, G P Karpacheva, R V Talroze, Y V Kudryavtsev

Contents

I.	Introduction	303
II.	Polymer – silicate nanocomposites	304
III.	Composites based on polymers and nanodiamonds	310
IV.	Electroconductive polymer composites	313
V.	Nanocomposites based on liquid-crystalline polymers	320
VI.	Conclusion	325

Abstract. Current challenges in the development of various polymer nanocomposites and in the study of their properties are considered. Results of studying hybrid structural (polymer – layered silicates, polymer – nanodiamonds) and functional (based on conducting or liquid-crystalline polymers) nanomaterials are presented. Methods of modification of nanoparticles and their dispersion in a polymer matrix, and the role of interactions between a polymer matrix and fillers, as well as of nanoparticle morphology realized in the course of processing, are discussed. The bibliography includes 453 references.

I. Introduction

Many natural and artificial structures fall within the nanometre range: clay mineral and latex particles (100 nm – 1 μm), polymer and DNA molecules, viruses (10 – 100 nm), protein and dendrimer molecules, metal and semiconductor nanoparticles (1 – 10 nm). These structures serve as building blocks for creating nanomaterials, which have significantly different properties as compared with those of materials composed of larger structural units. Design of nanomaterials and tailoring of their properties are the main task of the development of nanotechnologies; however, understanding the size effects and establishing corresponding relationships is impossible without fundamental interdisciplinary research.[1]

The present review focuses on polymer nanocomposites, an important class of nanomaterials, which have garnered significant interest since their inception in the late 1990s. As reported by Vaia and Maguire,[2] the number of articles and patents, as well as research and development funding, in this area has been growing exponentially. For example, the total number of hits for 'polymer nanocomposites' on SciFinder (Chemical Abstract Service of the American Chemical Society) from 1988 to 2005 is 9400, where the yearly number has approximately doubled every two years since 1992. In the last years, this growth has continued, even if at a slower pace than previously:

Years	2006	2007	2008	2009	2010	2011	1988 – 2011
Number of records	2995	3460	3863	4182	4910	5197	34 122

Polymer nanocomposites are polymers filled with particles that have at least one of the dimensions on the nanometre scale. In zero-dimensional (0D) nanocomposites, all three dimensions of the filler are on the order of 1 nm (spherical silicate nanoparticles,[3] metal and metal oxide nanoparticles,[4 – 6] detonation nanodiamonds,[7, 8] quantum dots,[9, 10] *etc.*). One-dimensional (1D) nanocomposites contain a filler nanosized in two dimensions (nanotubes,[11 – 15] fibres or whiskers [16]), and two-dimensional (2D) nanocomposites are layers of nanometre thickness (layered silicates,[17 – 19] metal chalcogenidies,[20] graphite,[21] *etc.*).

Nanocomposites can be divided by their application into structural and functional. For structural nanocomposites, the introduction of filler efficiently enhances their durability, inflammability, barrier properties and processability. Nanosized fillers with adsorbed substances are able in some cases to impart functional properties to structural compo-

V A Gerasin, V V Karbushev, G P Karpacheva, R V Talroze, Y V Kudryavtsev A V Topchiev Institute of Petrochemical Synthesis, Russian Academy of Sciences, Leninsky prosp. 29, 119991 Moscow, Russian Federation. Tel. (7-495) 955 41 54,
e-mail: gerasin@ips.ac.ru (V A Gerasin),
tel. (7-495) 955 42 55, e-mail: gpk@ips.ac.ru (G P Karpacheva),
tel. (7-495) 955 41 38, e-mail: rtalroze@ips.ac.ru (R V Talroze),
tel. (7-495) 954 22 85, e-mail: yar@ips.ac.ru (Y V Kudryavtsev)
E M Antipov Department of Fundamental Physical and Chemical Engineering, M V Lomonosov Moscow State University, Leninskie Gory 1, 119991 Moscow, Russian Federation. Tel. (7-495) 955 41 69, e-mail: antipov@ips.ac.ru
V G Kulichikhin Department of Chemistry, M V Lomonosov Moscow State University, Leninskie Gory 1, 119991 Moscow, Russian Federation. Tel. (7-495) 952 41 45, e-mail: klch@ips.ac.ru

Received 27 April 2012
Uspekhi Khimii **82** (4) 303 – 332 (2013); translated by G A Kirakosyan

sites, for example, biocidal properties or electroconductivity. Theoretical models of such composites are described by the laws of classical mechanics of solids and viscous fluids. For fabricating structural nanocomposites, it is necessary to create stable mixtures in which inorganic nanoparticles are well dispersed in the bulk of a polymer matrix, have no tendency to coagulate and (in the case of anisodiametric particles) are capable of orientation in the manufacture of products. Different methods of nanoparticle modification and nanocomposite production are used for this purpose. Studies in this field are surveyed in Section II for polymer–silicate nanocomposites and in Section III for polymer–nanodiamond composites.

The role of the filler in functional composites is much more significant since the electric, magnetic, optical and other properties of a material often depend substantially on the corresponding characteristics of nanoparticles.[22–25] Of great significance is the interaction between the filler and polymer matrix at the molecular level, which can lead to synergy of useful properties of the organic and inorganic components of a material.[26,27] For describing these interactions, quantum notions and models should be invoked. The possibilities of designing functional composites based on conducting polymers and fillers of different nature and dimension are considered in Section IV.

In some cases, especially for use in photonics and optoelectronics, not only dispersion of the filler but also formation of a prescribed spatial arrangement of nanoparticles is important.[28–32] Two general approaches to the design of 'organized' nanocomposites have been considered[2]: external-in, *i.e.*, directed patterning of nanoparticle dispersions, and internal-out, *i.e.*, mesophase assembly of nanoparticles. The potential of the first approach has been demonstrated by the example of uniaxial alignment of nanosized plate and sticks under sedimentation,[33] spin coating,[34] fibre spinning,[35–38] film blowing,[39] injection molding,[40] shear,[41,42] magnetic fields[43,44] and electrical gradients.[45]

Although directed patterning of nanoparticle dispersions makes it possible to achieve any filler distribution, real processes are limited by the time of pattern development in highly viscous polymer media and by the necessity of using special equipment to maintain structural precision on the submicrometre scale. In this context, a natural alternative to direct patterning of nanoparticle dispersion is the inherent organization derived from a thermodynamically well-defined phase. The potential of this approach is discussed in Section V for nanocomposites based on liquid-crystalline (LC) polymer matrices as a control medium for quantum dot alignment.

This review does not touch upon some important classes of polymer nanomaterials (for example, nanocomposites based on biopolymers). At the same time, the selection of subjects mainly caused by the scientific interests of the authors is rather wide and provides the insight into the progress and current problems in the area under consideration.

II. Polymer–silicate nanocomposites

It is typical that only a small portion of polymer materials consist of one substance. Polymer engineering has long been aimed at design of composite materials in which a required set of properties is achieved by a tailored combination of components. Polymer composites are a result of the search for optimal combinations of polymers and fillers of different nature. There are also natural materials of this kind: for example, wood is a polymer composite reinforced by oriented fibres.

The use of filled polymer materials enables the fabrication of radically new constructions and diverse articles and makes it possible to reduce their weight and improve their quality and appearance. The technology of fabrication of polymer articles is simple and efficient and is suitable for producing parts of complex shape.

For composites based on large-scale polymers, the most essential are mechanical properties responsible for their performance under operating conditions. The properties of filled polymers are determined by various factors:[46–48]

— the filler particle size;

— the particle shape;

— the orientation of particles and their mutual arrangement in a matrix (ordered or random, agglomeration);

— the degree of filling;

— characteristics of the polymer matrix (binder);

— the interaction between the filler and the binder (adhesion bond strength, the effect of the filler on the properties of boundary layers or polymer crystallization).

Elastomer-based composites containing micron-sized filler particles have, as a rule, enhanced stiffness, yield strength and thermal resistance;[49,50] however, in hard polymers, such fillers are usually not reinforcing. Moreover, they often significantly decrease deformability and impact resistance because of stresses that appear at the filler particle surface or in the polymer near this surface. The use of smaller filler particles improves the situation. In particular, for polypropylene (PP) nanocomposites, filling with silica leads to a considerable increase in the yield strength and Young's modulus (elastic modulus),[51] and filling with calcium carbonate[52] or montmorillonite (MMT)[53] increases the strength of the composite, no sharp decrease in the material elasticity being observed. It is worth noting that the introduction of only 5 mass % of clay into PP leads to the same strength of the composite material as the introduction of 20% of talc or 15%–50% of chalk.[54]

In composites with an elastomer binder, the use of nanosized fillers leads to an even more significant improvement of mechanical properties than for rigid polymer matrices. It has been shown that the sixfold increase in the elongation at break and the threefold increase in the elastic modulus of polyurethane (PU) is achieved by filling it with 40 mass % of silica with a particle size of 12 nm.[55,56] A noticeable strengthening of rubber used for tyre production is observed when filler particles have a specific surface of >50 m^2 g^{-1}, which corresponds to the spherical particle diameter <50 nm. Unfortunately, this general correlation (the finer the filler, the better the improvement of the mechanical properties of polymer matrices), including the case of large deformations, has not been mathematically formulated to date even for amorphous polymers. It should be taken into account that immediately after applying load and appearance of strain in the material, the polymer structure, orientation of filler particles and their connectivity change. For partially crystalline polymers, the pattern is even more complex.

The macroscopic deformation behaviour of filled highly elastic polymers with imperfect adhesion is caused to a great

extent by phase separation and micropore formation processes.[57–59] It has been shown that the stress required to cause debonding between a hard spherical inclusion and amorphous polymeric matrix is inversely proportional to the square root of the inclusion radius and increases with an increase in the elastic modulus of the matrix.[60]

The stresses that emerge near the filler surface upon composite loading interfere in polymer interlayers, which leads to an increase in local stresses in the matrix.[61] The decrease in the filler particle size leads to an increase in the minimal thickness of the interlayers and a decrease in the probability of the overlap of stress fields in them so that local overstress is reduced.

Both isodiametric particles (glass spheres, crumb rubber) and anisodiametric particles (fibres, nanotubes, plate-type filler) are used as a filler. To characterize the degree of anisodiametry of these particles, the notion 'shape factor' (geometric factor, aspect ratio) f is used. It is defined as the largest-to-smallest size ratio of the particles.[46]

Theoretical[62–66] and experimental[67,68] studies demonstrate that filler particles with a high aspect ratio have a stronger reinforcement effect on the polymer matrix as compared with isodiametric inclusions and particles with smaller f values. First of all, these are clay minerals consisting of colloid-sized particles capable of separating, under definite conditions, into essentially anisodiametric subparticles with one of the sizes being of the order of 1 nm.[69,70] The shape factor for MMT particles depends on the degree of their dispersion in the polymer (stacks or separate platelets) and can be as large as a few hundreds. In the past 15–20 years, different laboratories have synthesized nanocomposites based on dozens of polymers and layered silicates. Many of these composites have interesting properties. The results of these studies have been summarized in numerous reviews and books.[67,68,71–77]

Most of the publications focusing on design and properties of such materials deal with composites based on polyolefins (the worldwide production of polyolefins accounts for more than one-half of all produced plastics) and polyamides (PA). Typical examples are nanocomposites based on polyethylene (PE) or PP and a nanosized filler, layered silicate Na^+-MMT, which can be prepared by *in situ* polymerization[78,79] (so-called polymerization filling) or by melt compounding.[80,81]

Considerable interest in similar composites is caused by the effort to produce materials that would combine low cost with a set of properties superior to the properties of the neat polymers.

1. Properties of layered silicates and their modification

The unique nature of layered silicates determines both the problems and the great possibilities for creation of a wide spectrum of multifunctional composite materials.[82] The major units of the clay mineral structure are the silicon–oxygen ion SiO_4^{4-} and the aluminium–oxygen ion $Al(O/OH)_6^{3-}$ (Refs 69, 83 and 84). These structural units form, respectively, tetrahedral and octahedral two-dimensional networks capable of sharing oxygen ions to form layers (sheets) constituting the basis of the clay mineral. Depending on the tetrahedron-to-octahedron ratio in the layer, clay minerals are designated as 1 : 1, 2 : 1, 2 : 1 : 1, *etc.*[85,86] Natural layered aluminosilicates routinely used in nanocomposites are representatives of the 2 : 1 family (Fig. 1).

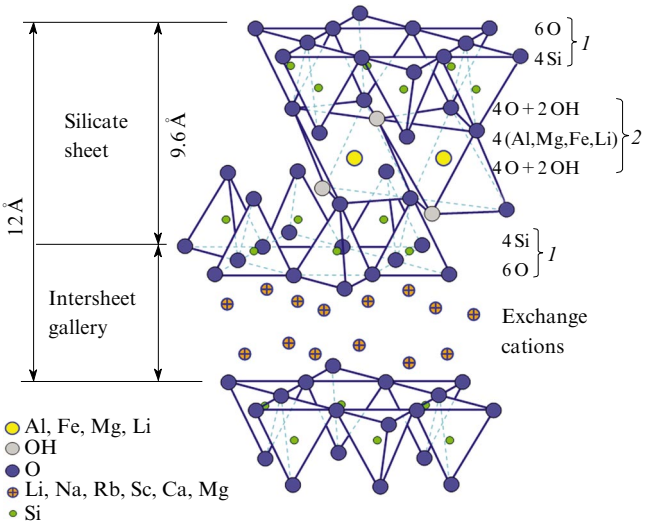


Figure 1. Schematic representation of 2 : 1 clay minerals.[69] (*1*) Tetrahedral network, (*2*) octahedral network.

The particle size in clay samples is determined by the degree of isomorphous substitution of Si and Al atoms, as well as by the nature of the substituent atoms. The distance between oxygen atoms is 2.60 Å in the octahedron and 2.55 Å in the tetrahedron.[69] Since these atoms are shared by the networks of both types, internal stresses appear in the sheets, which leads to limitation of their size. The aluminosilicate unit cell dimensions are $5.2 \times 9 \times 9.6$ Å,[87] and the sheet dimensions are $\sim 1000 \times 1000 \times 1$ nm.[69]

Owing to van der Waals interactions, aluminosilicate platelets self-assemble into stacks (tactoids) with regular 'passages' (intersheet galleries) between separate sheets distinguished by electron microscopy. The thickness of these tactoids is up to 50 nm, and the transverse size is up to 1–2 μm.

Isomorphous substitution inside the layers (when, for example, ions with a smaller charge, Mg^{2+} or Fe^{2+}, are substituted for Al^{3+} in the octahedral layer and Al^{3+} or Fe^{3+} ions are substitution for Si^{4+} in the tetrahedral layer) leads to that the elementary layers become negatively charged (from 0.5e to 1.2e per formula unit).[86,88,89] The gallery between MMT sheets accommodates metal cations (Na^+, Li^+, Ca^{2+}, *etc.*) compensating for the negative charge of aluminosilicate sheets.

An important characteristic of a clay mineral is the cation-exchange capacity (CEC), *i.e.*, the amount of exchange cations (expressed in mg-equiv) that can be replaced by cations of another type per 100 g of clay.[90] For layered silicates, the CEC is 10–150 mg-equiv. MMT has the highest CEC, 80–150 mg-equiv. Theoretically, CEC is a constant quantity; however, in reality, up to 20% of charge is located at sheet edges and changes with pH, electrolyte concentration and other characteristics of a medium.[91,92]

The external and internal surface of layered silicates is hydrophilic and polar. This facilitates wetting and penetration into intersheet galleries (intercalation) of both low- and high-molecular-mass compounds containing polar groups, such as acetone and its derivatives,[93,94] methyl methacrylate, proteins and natural amino acids[95] and other com-

pounds with hydroxyl[96,97] and nitrile[98] groups. MMT is equally efficiently intercalated with compounds containing ester groups,[99,100] due to their specific interactions with cations and hydroxyl groups on the surface of silicate sheets.

At the same time, the polarity of the silicate surface hinders the interaction of MMT with nonpolar and weakly polar polymers [polyolefins, polystyrene (PS), *etc.*] and prevents the uniform distribution of silicate platelets in the polymer matrix. In this case, for fabrication of a polymer–silicate nanocomposite, it is necessary to create conditions for dispersion of clay in the polymer, intercalation of macromolecules into galleries between silicate sheets or complete separation of clay tactoids into platelets (exfoliation). To this end, clays are preliminarily modified by different methods:

1) by ion exchange of clay cations for organic cations;

2) by adsorption onto the clay surface of poly(vinyl alcohol) (PVA),[101] polyacrylamide[102] and other water-soluble polymers, alkyl ketones (acetone, methyl ethyl ketone, diethyl ketone), methyl methacrylate,[48] acrylonitrile[103] and other compounds forming complexes with the clay surface or exchange cations;

3) by adsorption of anions, in particular, polyacrylates, onto the edges of silicate sheets,[104–106] which becomes possible at pH < 5 as a result of protonation of hydroxyl groups located at the edges ($Al-OH \rightarrow Al-OH_2^+$);[107]

4) by grafting organosilanes, for example, 3-aminopropy(triethoxy)silane, to the clay surface to form Si–O–Si bonds;[108,109]

5) by introduction of organic molecules capable of van der Waals or ion–dipole interaction with the clay surface, for example, alkylammonium cations, for which the affinity for clay decreases in the series $RNH^+ > RNH_2^+ > RNH_3^+$ and increases with an increase in the length of the ion aliphatic chain.[84]

Although selection of surfactants as clay modifiers requires a knowledge of the specific features of the clay mineral structure and is individual for each matrix polymer, cationic surfactants containing from 6 to 20 carbon atoms, for example, primary, secondary and tertiary amines converted into a quaternary form by the treatment with equimolar amounts of mineral acids, are most often used as modifiers. For example, the simplest alkylammonium cations Me_4N^+ and alkylamines $MeNH_2$, Me_2NH and Me_3N efficiently replace the Na^+ ions from MMT, making the clay mineral surface organophilic,[110,111] which ensures its compatibility with macromolecules. As organophilicity increases, water adsorption by clay is reduced.

When interlayer metal cations after ion exchange are replaced by bulkier organic cations, the interlayer distance increases, which can be judged from the small-angle shift of the basal reflections in the X-ray diffraction patterns of the clay.[112] Modification of layered silicates by surfactant adsorption on their surface also destroys the structural hierarchy of the clay formed by adhesion of separate silicate crystallites, which is accompanied by a decrease in the number of silicate platelets in the tactoid.

The modification-induced increase in the intersheet gallery of clay minerals depends on the charge of silicate sheets and the CEC of the silicate, the surfactant molecule size and shape, and the number and length of aliphatic chains.

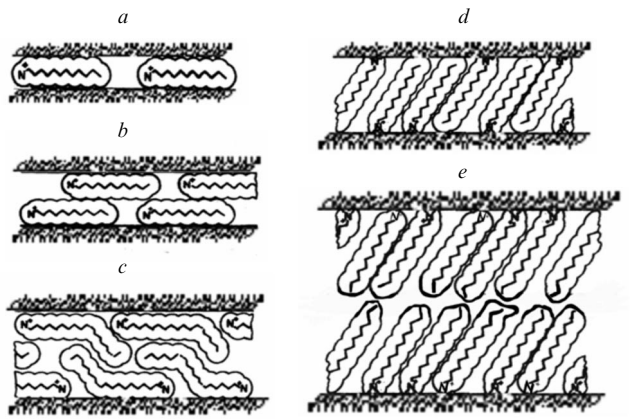


Figure 2. Structures formed by surfactants in the intersheet gallery of layered silicates: a horizontal monolayer (*a*), a horizontal bilayer (*b*), a horizontal pseudotriple layer (*c*), a paraffin-type monolayer ('pseudobilayer') (*d*) and a paraffin-type bilayer (*e*).[112,113]

Surfactants containing one aliphatic chain or having a planar molecular structure, such as n-butylamine, aniline and pyridine, are absorbed by the clay, forming one or two adsorption layers with parallel arrangement of chains (or rings) between silicate sheet planes (Fig. 2 *a*,*b*) and increasing the intersheet distances by ~0.6 nm.[114] Aminopyridines,[115,116] polyvinylpyridine,[117] polyaniline (PANI)[118] and acetonitrile[119] are also sorbed onto MMT, forming one layer and moving silicate layers apart by 0.5–0.6 nm. The sorption of saturated amine vapour by monmorillonite can lead to the appearance of the third adsorption layer with an increase in the distance between silicate sheets by 1.2 nm.[120]

A similar behaviour is observed for polyfunctional compounds. In particular, aminobutyric, aminocaproic and aminolauric acids are sorbed onto MMT and force clay sheets apart by 0.6 nm when taken in amounts not exceeding the CEC of the clay and by 1.2 nm when taken in excess.[114,121]

The ion-exchange sorption of Me_4N^+ and Et_4N^+ cations with a short aliphatic chain leads to an increase in the intersheet distance only by ~0.5 nm;[120] however, for a longer aliphatic chain of a surfactant, the number of adsorbed molecules being the same, this distance increases more significantly.[122,123]

The number of exchange positions on the silicate sheet surface determines the packing density of modifier molecules. At a large CEC of a clay mineral, primary amines with an aliphatic chain length larger than a definite length form so-called pseudotriple layers in the intersheet space (Fig. 2 *c*) so that the distance between silicate layers increases to 2.1 nm.[112]

Molecules of quaternary ammonium salts (QASs) containing two long aliphatic chains can form 'paraffin' mono- or bilayers, which are arranged in the interlayer space of MMT at a certain angle to the layered silicate surface and attached to the one or different sheets (Fig. 2 *d*,*e*).[113,124,125]

All types of layers are easily identified from X-ray crystallography data; however, according to mathematical modelling results,[126–128] these data are insufficient to determine the true structure of interlayer molecules. The inter-

layer structure and conformation of aliphatic chains of QASs intercalated into the interlayer space of silicate sheets are the objects of intensive study.[113, 129] The use of differential scanning calorimetry (DSC) and Raman spectroscopy in addition to X-ray crystallography significantly improves the reliability of results.[79, 129–131] It is worth noting that it is precisely the arrangement of modifier molecules in the intersheet gallery that determines the distance between silicate sheets, organophilicity of intersheet galleries of the clay and, ultimately, the structure of nanocomposites formed upon mixing the clay and polymers.

2. Synthesis and properties of polymer–layered silicate composites

The use of clays with different CECs, selection of modifying organic cations and tailored formation of organophilic layers taking into account the properties of the polymer matrix enables the fabrication of composites of several types (Fig. 3). For nanocomposite synthesis, it is necessary to destroy the entire hierarchy of morphological formations down to separate crystallites or even silicate platelets.

If the polymer is not intercalated in the space between the crystallite layers, a composite with separated phases is formed (**A** in Fig. 3 *b*), and its major characteristics are in the same range as those of common microcomposites.

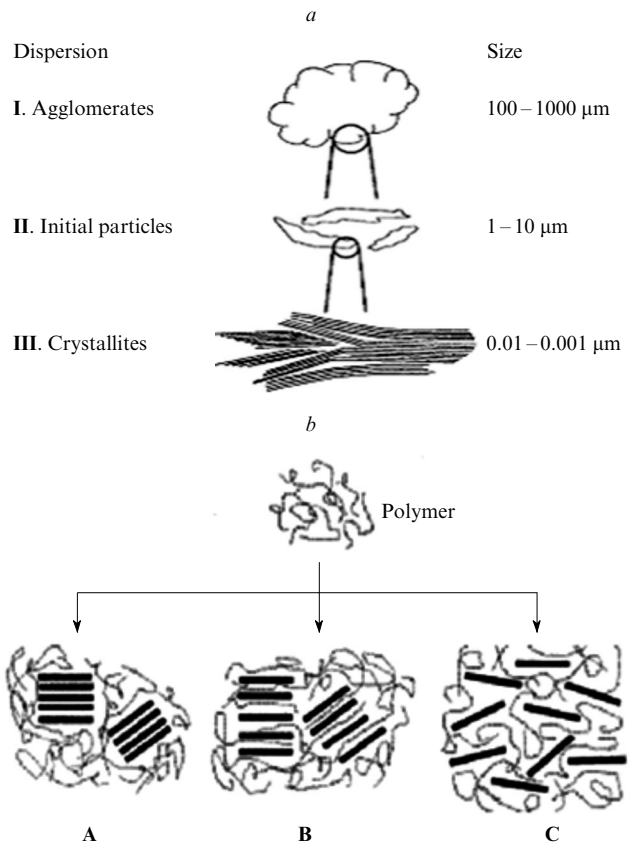


Figure 3. Schematic representation of morphological formations of the clay (**I**–**III**) (*a*) and the type of nanocomposite structures that appear through the interaction between layered silicates and polymers (*b*).[67]
A is two-phase microcomposite, **B** is intercalated nanocomposite, **C** is exfoliated nanocomposite.

Another type of composite (**B** in Fig. 3 *b*) has a structure in which separate extended polymer chains are intercalated into the intersheet galleries of the clay, thus forming a well-ordered system of alternating polymer and silicate layers. In the composites of the third type (**C** in Fig. 3 *b*), aluminosilicate layers are completely dispersed in the polymer matrix, giving rise to the so-called exfoliated, or delaminated, structure.[67]

The type of polymer–layered silicate composite can be determined by X-ray diffraction from the position of the basal reflection. The displacement of this reflection toward smaller diffraction angles than in the pattern of the initial clay is evidence of the existence of a regular multilayer structure typical of intercalated nanocomposite. The disappearance of diffraction peaks can be due to the large (more than 8 nm) distance between layers or because of disordering in silicate platelets typical of completely exfoliated composite. The decrease in the reflection intensity is characteristic of a nanocomposite with partially exfoliated structure.

The type of composite and the filler dispersion degree can be determined by transmission electron microscopy (TEM);[132] however, this requires to examine a large number of images and use sample staining, which cannot be done for all systems. The exfoliation degree can be estimated by rheological techniques[133–135] by measuring the power-law coefficient of the viscosity *vs.* shear rate dependence, which characterizes the dispersion degree of the filler in composites.

The first attempt to theoretically describe intercalation of macromolecules into the intersheet galleries of the clay with surfactants adsorbed onto silicate platelets has been undertaken by Vaia and Giannelis.[136, 137] In terms of the mean-field theory, an expression has been derived for the change in the free energy of the system consisting of a modified layered silicate and a polymer melt. In the course of nanocomposite formation, the modifier molecules acquire greater conformational freedom as the layers separate, whereas macromolecules go from the melt into a narrow gap and experience the confinement effect of the walls. The overall change in the entropy of the silicate–modifier–polymer system is negative; therefore, for a thermodynamically stable nanocomposite to form, it is necessary that the energetic interactions should compensate for the entropic barrier. Otherwise, phase separation of components will occur so that a common microcomposite will form. Thus, the polymer ability to intercalate into layered silicates and conformations of macromolecules in two-dimensional space are determined, first of all, by the polymer polarity.[138, 139]

Further theoretical studies of the thermodynamic properties of the silicate–modifier–polymer melt system have been carried out by self-consistent field theory and density functional theory methods.[138, 140–144] The interaction between the system components has been described by means of pairwise energy parameters. The calculations suggest that the increase in the chain length of modifier molecules promotes the formation of thermodynamically stable nanocomposite. In this case, better interpenetration of the polymer and modifier molecules is observed, which increases the conformational freedom of both components. Therefore, for exfoliation of layered silicates in nonpolar polymers, in addition to clay modifiers, comodifiers with

polar groups and long aliphatic 'tails' capable of penetrating the polymer matrix are often used.[145, 146]

In recent years, works aimed at creating multilevel models of polymer nanocomposites relating molecular parameters to the macroscopic properties of the system have been carried out.[147–152]

Polar water-soluble polymers — PVA,[153, 154] poly(ethylene oxide) (PEO),[154, 155] poly(ethylene glycol) (PEG),[156–159] polyvinylpyrrolidone,[160] and poly(acrylic acid)[158] — as a rule, spontaneously intercalate into clay galleries. Nanocomposites are fabricated by adding polymer solutions to dispersions of swollen layered sodium silicates in water or organic solvents. For example, PEO has been successfully intercalated into sodium MMT and hectorite from acetonitrile.[161]

Intercalated nanocomposites are also obtained by means of polymer synthesis and modification reactions. Poly(methyl methacrylate) (PMMA)–clay[162] and PS–clay[163] nanocomposites have been produced by emulsion radical polymerization, and clay–polyimide composites have been prepared by mixing modified MMT with poly(amido acid) in dimethylacetamide and heating the mixture to 300 °C.[164] According to X-ray diffraction, under equilibrium conditions, the interlayer spacing nearly always increases only by the polymer monolayer.

At present, the mechanisms responsible for the increase in interlayer spacing cannot be clearly distinguished. When a polymerization filling technique is used, the increase in the interlayer thickness and the extent of silicate platelet exfoliation are determined by many factors, in particular, diffusion kinetics of monomers and the change in their concentration during polymerization, the interaction of monomers with the filler surface and the type of surfactant used for clay modification.[122]

Under certain conditions (the polymer-to-clay ratio is large and polymerization occurs in the prepolymer melt), the X-ray diffraction patterns of the composites do not show peaks typical of the intercalated structure, which can be interpreted as evidence of exfoliation.[165]

Polymerization of ε-caprolactam with ring opening afforded nanocomposites containing MMT modified with 12-aminolauric acid.[166, 167] According to XRD and TEM, formation of an exfoliated (clay content < 15 mass %) or intercalated (15 mass %–70 mass % clay) structure depends on the filler content.

Polar oligomers, for example, epoxy resins cured with maleic anhydride (MA), form with clay completely exfoliated nanocomposites.[168]

It is more challenging to produce nanocomposites based on nonpolar or weakly polar polymers. It has been demonstrated in numerous studies that, under equilibrium conditions, PE,[169] polylactides,[170] poly(ε-caprolactones)[171] or PS kept under pressure in melt at temperature above the polymer softening point[172] are unable to spontaneously intercalate into clay galleries, whatever the modifier is used. Partial intercalation is achieved by modifying the polymer to increase its polarity (chlorination of PS[172]) or using severe conditions of composite preparation (treatment of the clay with high-boiling organic solvents and its extrusion together with the polymer at high temperature[173]). The use of a comodifier (usually a functionalized low-molecular-mass polyolefin) is more efficient and makes it possible to produce both intercalated and exfoliated nanocomposites.[174–182]

Nanocomposites based on nonpolar polymers can be synthesized without introducing comodifiers if the polymer–clay mixture is formed under thermodynamically nonequilibrium conditions. Such conditions can be realized for polymerization of nonpolar or weakly polar monomers over clay-supported catalysts. If the polymer formed in clay galleries is insoluble in the reaction medium at polymerization temperature, the entropic and enthalpic barriers to intercalation of the nonpolar polymer into polar silicates are removed. To this end, it is necessary to create conditions for clay swelling in the reaction medium, which provides access into clay galleries for the catalyst and monomer.[78] This is possible for surfactant-modified clay. When a certain molecular weight is achieved, the resulting polymer is deposited in clay galleries, separating silicate platelets.

Exfoliated and intercalated nanocomposites based on PE of different density have been synthesized by polymerization of ethylene and long-chain α-olefins on various catalysts with the use of modified clays.[183] The PE–MMT and PE–hectorite composites have been synthesized on the MAO (methylaluminoxane) catalyst preliminarily applied to unmodified clay in suspension in hexane and xylene.[184] The same catalyst, along with bifunctional clay modifiers based on alkylaluminium and vinyl alcohol, has been used for preparing exfoliated nanocomposites.[185] The copolymerization of vinyl groups with ethylene leads to that the modifiers are fixed into the silicate galleries.

Exfoliated nanocomposites have been fabricated by ethylene polymerization or ethylene–1-octene copolymerization in neat Na^+-MMT on the $MgCl_2/TiCl_4$ catalyst activated with $AlEt_3$,[186] and in clay modified with L-amino acids or a complex modifier (L-amino acid–cetyltrimethylammonium bromide) on the zirconocene catalyst.[187] The elastic modulus, strength, creep, yield point and other essential engineering characteristics of materials are measured by mechanical analysis methods.[67, 68, 84]

The elastic modulus of the PP–modified MMT nanocomposites containing only 1 mass % clay was found to be eightfold higher than that of the neat PP.[188] At the same time, a noticeable increase in the composite strength was observed at clay contents no lower than 10%. The composites also exhibited enhanced crack resistance: at the filler content 10 mass %, the time to failure exceeded that for the neat polymer by a factor of 4.5.

The elastic modulus can be additionally increased with the use of a modified filler. In particular, for nanocomposites based on Nylon-6, saponite particles and 12-aminododecanoic acid-modified MMT obtained by intercalation polymerization, the elastic modulus at 120 °C increases with an increase in the filling degree in the range 0%–7.5%.[189–191] It has been demonstrated that the increase in the elastic modulus is proportional to the average length of layers of dispersed nanoparticles. For analogous composites containing up to 18 mass % clay, the elastic modulus monotonically increased up to the clay content 10 mass %, and then its growth became slower.[192] As follows from DXR and TEM data, at this clay content there is a transition from the completely exfoliated structure to the intercalated–exfoliated structure. Thus, the composite elasticity depends not only on the concentration of layered silicate particles but also on the degree of their exfoliation.

The mechanical properties of a nanocomposite depend on the nature of the clay–polymer adhesion bond.[189] For the systems based on maleic anhydride-modified PP and PP

oligomer (PP-MA) prepared by melt intercalation, the increase in the PP-MA content leads to an increase in the intercalation degree up to partial exfoliation and to the corresponding increase in Young's modulus.[175] For the nanocomposites based on weakly polar PMMA[160] or PS[193] synthesized by emulsion polymerization in the presence of water-swollen Na^+-MMT, Young's modulus increases insignificantly: from 1.21 to 1.30 GPa when 11.3 mass % of the filler is introduced.

A considerable increase in the interplanar spacing (to 7 nm) in nanocomposites obtained by polymerization filling of epoxy resins with montmorillonite does not lead to a noticeable increase in their elastic modulus.[123] As stated by Zilg *et al.*,[168] the material toughnes is caused by specific features of supermolecular entities appearing in the presence of anisotropic nanoparticles. It has been shown that the toughness of epoxy nanocomposites cured with anhydrides changes only slightly upon the formation of a properly exfoliated structure; however, the use of amino acids or amino alcohols leads to the increase in the elastic modulus of the composite.

Another significant characteristic of physical and mechanical properties of polymer–silicate nanocomposites is strength. In general, the strength builds up with a decrease in particle size, although anisotropy of filler particles in the exfoliated structure can be a detrimental factor because of local stress concentrations.[194]

In thermoplastic-based nanocomposites, the strength depends strongly on the nature of interaction between the matrix and filler. Nylon-6-based exfoliated systems prepared by different methods[189–191] or PMMA-based intercalated systems[195] exhibit enhanced strength, which is commonly explained by ionic or polar interactions between the polymer and silicate layers. The strength enhancement is more pronounced in Nylon-6-based composites, which have an exfoliated structure and are characterized by ionic bonds between the polymer and silicate. Ion–dipole interactions in the case of PMMA or PS (induced dipoles)[163] in intercalated nanocomposites do not afford a significant increase in material strength.

In PP-based nanocomposites, the gain in strength is either small or absent. Such a behaviour can be explained by the insufficient adhesion between the nonpolar polymer and polar layered silicates where the filler particles either play a passive role, exfoliating from the matrix, or even serve as the centres of defect formation.[196] The introduction of a small amount of PP-MA into the nanocomposite promotes the intercalation of polymer chains and increases the strength.[174] Preliminary treatment of the filler with, for example, functional silanes have an analogous effect.[188] A small increase in strength is also observed for intercalated PE–clay systems prepared by polymerization filling.[184]

The effect of formation conditions and nanocomposite structure on yet another essential characteristic of nanocomposites — elongation at break — has been little studied to date. It has only been stated that, for intercalated systems based on PMMA,[195] PS[163] and PE[184] or for the intercalated–exfoliated PP-based composite,[174] the elongation at break decreases by 5%–10%.

The behaviour of nanofillers with significantly anisodiametric shape is determined, first of all, by the strength of 'squeezing' of macromolecules in clay galleries,[197] which is fundamentally different from the case of the 'classical' filler. Depending on the tactoid orientation with respect to the external loading direction, the ends of filler sheets can move relative to each other, thus facilitating the exit of polymer chains from the galleries, or come closer together, thus holding the intercalated macromolecules.

The interaction between macromolecules and silicate particles has a strong effect on the rheological properties of the composite. Polymer filling with disperse particles is usually accompanied by an increase in system viscosity; however, for PVA–MMT composites (up to 5 mass % clay) the viscosity decreases by a factor of 2.7.[97] At high shear rates or upon prolonged exposure to low-rate shear, silicate platelets in polymer melts or greases are aligned parallel to the applied load, which leads to a considerable decrease in melt viscosity[133] and texturing of the silicate filler in the composite.[80, 198, 199] It follows from data on the glass transition temperature and polymer chain conformation[200] that the decrease in the viscosity of particulate-filled PP nanocomposites is accompanied by the increase in free volume.

Theoretical studies of a continuum hydrodynamic model[201–203] have enabled the prediction of the decrease in the composite viscosity even for spherical particles of a nanofiller. The model attributes this effect to the dynamics of polymer chains at the nanoparticle–polymer interface. The decrease in the amount of macromolecules in the polymer layer at the filler–polymer interface leads to the local reduction of the layer viscosity, which facilitates the movement of particles in the polymer matrix.[201, 202] If the regions with reduced polymer viscosity start overlapping (according to Ref. 204, efficient interaction between the filler particles appears when the average distance between them is twice as small as the gyration radius of the polymer chain), the resistance to flow of the polymer–filler system is additionally reduced.[205] If the polymer depletion layer thickness is more than the nanoparticle radius and its viscosity is lower than the polymer viscosity, the intrinsic viscosity of the composite becomes negative.[203]

It is worth noting that significant changes in viscoplastic and rheological properties of various polymer nanocomposites occur at small filler contents in the system (5 mass %–10 mass %).

For composites based on PA-12, PS and maleinized PS and PE, the increase in the dynamic modulus of the materials is especially significant at low frequencies: it exceeds the corresponding modulus values for neat polymers by 2–3 orders of magnitude in the case of PA and PS and by two orders of magnitude in the case of maleinized PE.[206, 207]

Study of dynamic properties has shown that, for polycarbonate (PC) containing 4.5 mass % of modified MMT, the dynamic modulus is 2–3 orders of magnitude higher than that for neat PC at low frequencies but is lower than the latter at high frequencies.[208] The dynamic modulus values substantially depend on the type of organic cation.

The rheological properties of nanocomposites based on layered silicates depend on the molecular mass of polymers and the degree of intercalation of polymer molecules into clay galleries. In particular, the increase in the dynamic loss modulus and especially dynamic elastic modulus is observed in the PP–MMT system.[207] The rheological properties of composites based on ethylene–vinyl acetate copolymers containing the clay mineral fluorohectorite treated with a modifier — a mixture of $(n\text{-}C_{18}H_{37})Me_3N^+$ cations and protonated aminolauric acid — have been studied.[209] It turned out that the dynamic modulus of the composite with

separate phases does not noticeably increase, whereas the modulus of the exfoliated system at low frequencies increases by two orders of magnitude.

Among other promising characteristics of polymer–silicate nanocomposites are the decreased gas pemeability, enhanced heat and fire resistance, high ion conductivity and low thermal expansion coefficient. The high adsorption capacity of the clay enables its use as a carrier for different substances that should be uniformly distributed in the polymer. This can be exemplified by composites based on MMT modified with different guanidine copolymers, which have pronounced biocidal properties.[210]

Nanocomposites of thermoplastic polymers and layered silicates are already commercially available and applied in automotive industry and packaging industry. They became a new and very promising class of materials due to the simplicity of their fabrication. At the same time, the increased interest in nanocomposites has not yet led to an abundance of commercial products. First, this is due to the fact that the filler exfoliation achieved in many polymers did not lead to the significant improvement of the mechanical properties of composites, except elastic modulus. Second, the requirements for high dispersion of the filler and its uniform distribution in the polymer matrix necessitate modification of existing production processes, which greatly increases the cost of production.

In this context, basic research in this area is essential. It is hopeful that deeper insight into the principles of formation of polymer–silicate nanocomposites will make it possible to formulate new ideas and strategies capable of giving impetus to development of modern technologies for creation of materials based on these systems.

III. Composites based on polymers and nanodiamonds

From the widest range of nanoparticles, detonation nanodiamonds (DND) with excellent physical and mechanical properties[211,212] are promising candidates for use as polymer modifiers. The detonation synthesis of nanodiamonds was discovered in the USSR in 1963.[212] The developed process of DND production currently involves detonation synthesis from explosives with a negative oxygen balance.[213,214] DND particles are, on average, 4–6 nm in size. Detonation nanodiamonds have a cubic crystal lattice with the unit cell parameter $a = 0.355$ nm, the density 3.05–3.4 g cm^{-3} and local microstresses $\sim$10 GPa.[213]

Since DNDs are synthesized under nonstationary, extremely severe explosion conditions, the particles have no common surface composed of carbon atoms combined into a crystal structure; rather, they have a 'fringe' of oxygen-containing functional groups (Fig. 4). In particular, in addition to carbon, DNDs contain considerable amounts of heteroatoms, and their content depends on synthesis, purification and processing conditions. On average, DNDs contain 80%–88% carbon, which is mainly in the diamond phase. They also contain oxygen (10% or more), hydrogen (0.2%–1.5%), nitrogen (2%–3%) and noncombustible residue (0.5%–8.0%) composed of oxides, carbides and salts of different metals, such as Fe, Ti, Cr, Cu, K, Ca, Si, Zn and Pb.[7,216] These compounds, along with non-diamond carbon, are difficult-to-remove solid impurities. This is responsible for a set of unusual properties and uncommon applications of detonation nanodiamonds.[215,217,218]

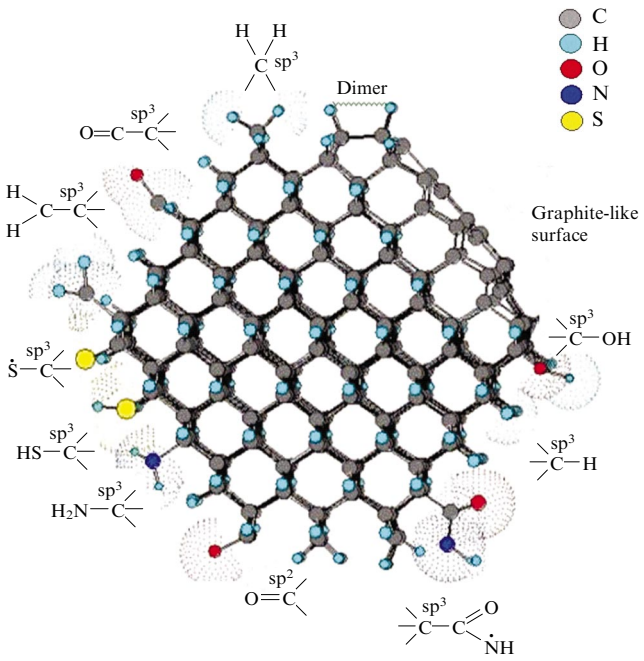


Figure 4. Schematic structure of the DND particle with different functional groups.[215]

IR spectroscopy indentifies various functional groups on the DND surface after processing under different conditions: oxygen-containing (hydroxyl, carbonyl, ester, anhydride, *etc.*), nitrogen-containing (amide, amino, cyano and nitro groups, *etc.*), sulfo groups, *etc.*[7,216] In addition, methyl and methylene groups are identified on the particle surface, but their content is insignificant. DNDs also contain bound and sorbed water, which is not removed even on drying the powders at 393 K. It is evident that this water is immobilized in closed pores formed in the course of DND synthesis.

An important problem is the necessity to tailor the surface properties of purified nanodiamonds since it is precisely the surface composition that predetermines their application to different fields. The nanodiamond surface is modified by various methods, including heat treatment of a suspension or chemical treatment in different media at high or low temperature. This essentially changes the ratio of hydrophilic to hydrophobic groups on the diamond surface, sorption properties, surface charge, *etc.* Nuances of DND fabrication process, chemical purification and modification may have a strong effect on both the physical and chemical properties and the performance of diamonds in composite materials and coatings. Different methods of particle surface modification have been developed that allow obtaining the type of DND most suitable for a certain field of application.[219–224]

DND nanoparticles have a very high surface energy and, therefore, form difficult-to-destroy blocks (clusters) 200–300 nm in size, which are combined in bulkier amorphous aggregates. Depending on the nature of the functional cover, colloidal properties of DND significantly vary. DND particles aggregate in both dry powders and suspensions, thus forming stable primary (up to 1–5 μm) and less stable secondary (up to 200 μm) aggregates,[216,225] and in liquid polar media, which significantly limits the possibility

of achieving the properties predicted on the basis of the size of individual nanoparticles. For some practical purposes, DND suspensions in nonpolar media should be used; however, the DND surface is hydrophilic[226] and is not solvated by low-molecular-mass liquids of this type.

High-priority uses of DNDs are in electrochemical and chemical metal–diamond coatings,[214, 222, 227–230] polymer–diamond composites (films materials, membranes, rubbers, plastics), additives to lubricating oils,[214, 222, 227, 228] polishing systems, diamond ceramics and toolware (electronics, cutters);[214, 222, 228, 231, 232] they are also used in medicine (gastric and antitumour drug carriers, immobilizers, adsorbents, *etc.*).[223, 231, 233–238]

Notwithstanding the fact that, in the above fields, polymer composites account for only a few percent of used DNDs, this direction of their application is extremely promising. In technological processes intended to create new materials with the use of DNDs, they are assigned the role of strong structuring agent. A common feature of these processes is the very low consumption of nanodiamonds (often a fraction of a percent), while the beneficial effect is achieved by a change in the properties of the product through a change in the characteristics of the corresponding process in the presence of DNDs, be it polymerization, lubricating film formation, coating adsorption and formation, electrochemical metal deposition or polymer reinforcement. As a result, the structure of the final product can be modified so that its performance properties change dramatically.

Nanodiamond-modified polymers can be used in aircraft, automotive, tractor and shipbuilding industry; medicine; chemical and petrochemical industry; production of seals and shut-off valves for various purposes; and in protective and anti-friction coatings.[7, 225, 228]

Nanocomposites based on DND and polymers (rubbers) have been described for the first time.[8, 239] Owing to the nanometre size of the filler particles, these materials exhibit much better physical and mechanical properties than the neat polymers of common (micrometre scale) composites.

In some cases, modification of polymers and their blends with nanoparticles provides unique tribotechnical properties owing to formation of adsorption layers with a spatial network of physical bonds at the polymer matrix–nanoparticle interface.

As shown,[240, 241] the crucial factor is the method of introduction and dispersion of DND into polymer matrices since it is precisely the morphology of composites that has a decisive effect on their final properties. An original method of combination of a polymer with a filler has been proposed:[240] immobilization of DND particles on the polymer powder surface occurs in a cavitating inert medium (hexane) under ultrasonication with subsequent filtration and drying of the composite powder.

From the technological viewpoint, a rheological method of combination of the polymer and filler is more promising. In this method, nanoparticles are mixed with the polymer melt in elastic turbulence ('spurt') regime, which leads to the efficient destruction of DND agglomerates and their uniform distribution in the polymer bulk.[241] The use of high-speed equipment makes it possible to obtain nanocomposites containing more than 90 vol.% of particles < 100 nm in size (Fig. 5).

The thus produced composites based on DND and thermoplastics — the styrene–acrylonitrile copolymer

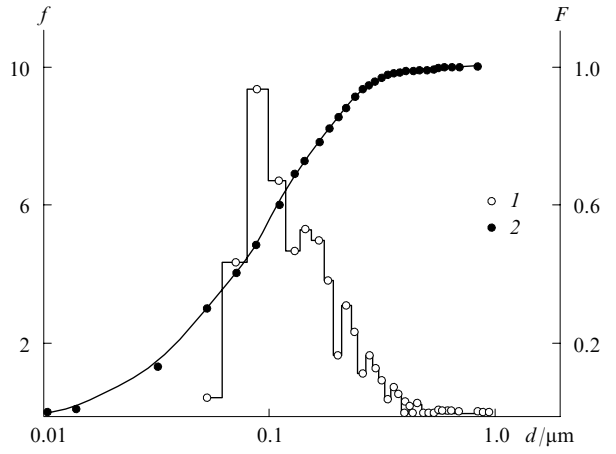


Figure 5. Differential (*f*, *1*) and integral (*F*, *2*) size distribution curves of DND particles (*d*) for the SAN–DND composite (1 mass %) obtained by melt mixing in spurt regime.[242]

(SAN) and polysulfone (PSF) — exhibit a set of improved properties. In particular, at the DND content 0.5 mass % in SAN, the elastic modulus and tensile strength increase by more than 30%, which is accompanied by the increase in impact toughness and hardness. The introduction of 0.5 mass % DND into PSF leads to an increase in impact toughness by 80%, whereas, in the composites containing 5 mass % DND, the Brinell hardness increases by 40% and the elastic modulus, by 100%.[241] Modifying DNDs with hexafluoropropyl alcohol improves their dispersion in PSF, which provides enhanced mechanical properties.[243]

It is interesting that the viscosity of thermoplastic melts with small additions of DNDs is reduced,[242, 243] which can facilitate the processing of composites into finished articles. Besides applied problems, the polymer melt viscosity reduction upon the introduction of a certain amount of nanoparticles has a fundamental significance since it reflects the change in the flow mechanism, especially at high rates — transition from segmental to stratified (layered) flow. Such a transition also causes the change in the morphology of a heterophase composite since a strong flow meets the conditions of precursor processing into a real nanocomposite. This circumstance compels us to consider rheological factors as key ones in synthesis of nanocomposites with tailored morphology.

The introduction of DNDs into thermoplastic PC leads to an increase in elastic modulus and a decrease in elongation at break. It has been demonstrated that, in the DND concentration range from 0.74 vol.% to 1.2 vol.%, the deformation behaviour changes from plastic to brittle before reaching the yield point. The cause for this change has been stated to be the formation of percolation cluster of fractal structure by DND particles.[244]

The use of DND as a component of oriented nanocomposites seems to be rather promising. This is due to the fact that nanodiamonds form extended indestructible aggregates capable of acting as efficient modifiers of physical and mechanical properties of polymer fibres. In particular, of interest is the attempt to design an oriented PVA-based composite (fibre) that would contain detonation nanodiamonds as nanosized filler.

PVA composites reinforced with DND particles have been synthesized by a solution method.[245] DND particles were functionalized to create surface carboxyl and hydroxyl groups by treatment with sulfuric and nitric acids. As the filling degree increases from 0 mass % to 0.6 mass % DND, the degree of crystallinity of the composites increases from 42% to 56%, while the elastic modulus and hardness increase twofold. Gel spinning conditions and regimes have been determined for producing PVA–DND nanocomposite fibres with considerably higher longitudinal elastic modulus values (the twofold increase, from 11 to 22 GPa, while the tensile strength remains constant) as compared to nonmodified polymer fibres.[246]

Epoxy adhesives filled with DNDs have good adhesive and cohesive properties. The use of DNDs in epoxy binders of glass fibre reinforced plastics efficiently decreases the longitudinal wear (a nearly twofold decrease is achieved at 10% DND).[247, 248] Minor amounts of DND (0.125 mass %) lead to a 50% increase in crack resistance of ED-22 epoxydiane resin and enhance its microhardness.[224]

Small DND additives to polyimide matrices increase the thermal degradation temperatures (by up to 30 °C). The introduction of 2 mass % DND into PA increases thermal conductivity by 15%,[249–251] and the microhardness of the composites increases by 15% and 26% at a filler content of 1 mass % and 5 mass %, respectively,[252]

The introduction of 0.24 vol.% DND into poly(ester urethane) plasticized with nitroglycerin leads to a twofold increase in elongation at break and a ~60% increase in tensile strength, while the elastic modulus remains constant or slightly decreases. It can be suggested that the fractal structure of nanodiamond clusters is responsible for the improvement of mechanical properties.[253]

Coatings based on Nylon-11 reinforced with DNDs produced by high-velocity oxy-fuel combustion spraying exhibit enhanced adhesion to a steel substrate, but inferior mechanical characteristics (elastic modulus and hardness), which is attributed to a nonuniform distribution of the filler in the matrix.[254]

The introduction of up to 1 mass % DND into epoxy resin (Epicote 827, Epicure curing agent, ASTRA) by ultrasonicationc leads to a more than 100% increase in the hardness of cured composites containing 0.67 mass % DND. The dielectric permittivity of the composite is reduced from 5.74 to 4.27.[255]

Polyacrylonitrile (PAN) and PA-11 nanofibres containing up to 80 mass % and 40 mass % DND, respectively, have been prepared by electrospinning.[256] Thin films of these composites can be used as UV protectors and protective coatings. In particular, for the PA-11 composite containing 20 mass % DND, a fourfold improvement of elastic modulus and a twofold increase in hardness are observed.

Composite films based on the ethylene–1-octene copolymer with 5 mass % DND have been obtained from solution.[257] DSC demonstrates that DNDs increase the degree of matrix crystallinity. The tensile strength of the composites increases from 3 to 5.1 MPa after material relaxation at room temperature for a month.

The efficiency of the introduction of DNDs into elastomers has been demonstrated by different researchers. In particular, filling fluoroelastomers with DND particles in the course of cold cure affords coatings with the following advantages:[7, 212]

1. The permeability to hydrocarbons and polar solvents decreases by a factor of 30–50. The highest chemical resistance in salt, acid and alkaline media is exhibited by filled copolymers of ethylene with perfluoroalkyl vinyl ethers (protective coatings).

2. The dry friction coefficient against metal decreases to 0.01.

3. Elastic and strength parameters are enhanced: the elastic modulus at 100% elongation and conventional tensile strength increase more than tenfold, which is accompanied by an increase in elongation at break by a factor of 1.6.

4. The contact adhesion strength increases, by 300%–500% for active surfaces (steel St3, zinc, aluminium).

Film coatings based on DND-modified polysiloxanes have noticeably better elastic and strength characteristics: there is an approximately threefold increase in stress at 100% strain (from 19 to 53 MPa), tensile strength (from 52 to 154 MPa) and elongation at break (from 730% to 1970%), while the tear resistance increases by a factor of 1.4.[7, 212]

On the basis of fluoropolymer–DND composites, a film-forming material has been developed for antifriction coatings of metal surfaces; this material has shown the dry friction coefficient against metal previously unattainable for polymers, <0.01. The developed process of hot curing of commercial polymers with DNDs provided the improvement of mechanical, antifriction and protective properties of composite materials and enhancement of their wear and radiation resistance. The DND content in such composites was from 0.1 mass % to 2.0 mass %.[7]

DND-modified fluororubbers have improved elastic and strength characteristics and are resistant to thermal ageing: the stress at 100% strain increases by 1.6 times (from 7.9 to 12.5 MPa), the tensile strength increases by 1.1 times (from 15.4 to 16.5 MPa), the relative elongation at break increases by 1.35 times (from 210% to 285%).[212] The abrasive wear resistance of DND-modified fluoroelastomers increases by a factor of 1.5–2.0, and in this characteristic, they are close to isoprene rubbers.[212]

The use of fillers modified by silylation (DNDs and technical diamond–carbon powders, superfine silica A-300, glass spheres) improves the mechanical properties of films obtained from suspensions of a filler in toluene solutions of polysiloxane block copolymers, by 20%–30% in the practically important strain range (up to 300%) with retention of satisfactory elastic properties.[258] It should be emphasized that such an effect is achieved at a filling degree of no more than 5 mass %.

The introduction of 0.05 mass % of aminated and silylated DNDs dispersed in polyol into the foamed polyurethane synthesized by polycondensation of polyol and diisocyanate increases the adsorption capacity of the material by 42% and enhances its strength.[259]

The mechanical characteristics of DND-containing rubbers remain roughly constant in the course of thermal ageing at 523 K, either being at the level of analogous characteristics of standard compositions (not subjected to heating) or exceeding them. The presence of DNDs is favourable for structuring rather than destructive changes in the composites in the course of thermal aging.

For polyisoprene rubbers, the introduction of modified DNDs leads to considerable improvement of elastic and

strength characteristics. In particular, for SKI-3 synthetic isoprene rubber, the stress at 300% strain increases by a factor of 1.6 (the same result is observed for SKI-5 rubber), conventional tensile strength increases by 1.4 times (from 20.5 to 28.2 MPa), and the tear resistance increases from 139 to 148 kN m^{-1}. The maximal swelling degree of the rubbers in toluene is reduced by 45%. These rubbers have higher crosslink density, strength characteristics ($\sim$30% higher than those of common rubbers based on SKI-3) and fatigue strength.[260] The increase in percent elongation with an increase in the elastic modulus of such rubbers is not consistent with generally accepted notions. This points to a change in the supermolecular structure of rubber, which is also supported by the significant increase in cohesion strength (from 1.7 to 2.7 MPa).

The introduction of DND into a standard SKMS-30 ARK rubber mixture based on the butadiene–styrene copolymer containing 30% styrene units increases the cohesion strength of the composite by a factor of 1.5–2.0. DND-modified rubbers are distinguished by the high degree of vulcanization, their strength characteristics being almost the same as for the reference rubber and their tear resistance being two times higher than that of the latter. The stress at 300% strain increases by a factor of 1.4.[260]

DND-modified butadiene–nitrile rubbers B-14 have improved performance characteristics: friction coefficient decreases by 1.5 times, wear resistance increases by 1.3 times and elasticity, by 1.7 times; frost resistance also increases (the glass transition temperature decreases by 8%–10%). For RSS natural rubber (Malaysia) modified with DND, stress at 300% strain increases threefold (from 1.8 to 5.4 MPa), its performance characteristics being somewhat improved. The friction coefficient against polyfluoroelastomers (such as copolymers of vinylidene fluoride with perfluorinated comonomers, *e.g.*, hexafluoropropylene) and perfluoro polymers is low, and that against polyisoprenes (SKI-3 and SKI-5) is high.[7, 239, 261]

Upon the introduction of 0.1 mass % to 2 mass % of diamond blend into commercial explosive decompression-resistant rubbers, the elastic modulus increases to 8 MPa, and tear and wear resistances also increase by 60% and 40%, respectively.[262]

On the whole, the enhancement of mechanical properties of polymer–nanodiamond composites is associated with that the decrease in the DND particle size is accompanied by the increase in the fraction of interfacial adsorption layers that have higher density owing to orientation of macromolecules in the field of nanoparticles as compared to the polymer in the bulk.[241] The fraction of the polymer component that undergoes structural and conformational transformations in the field of these particles is, in general, equivalent to the volume fraction of the wall boundary layer. It is assumed that the modifying effect can be significantly increased at a higher level of DND dispersion in the polymer matrix, which accounts for the fact that formulations of composites of different nature and preparation method differ in the nanodiamond content.

The tribological properties of polymer–nanodiamond composites have received considerable attention of researchers. It has been shown that DND is the most efficient additive for decreasing the wear rate of polytetrafluoroethylene as compared with well-known analogues.[247, 263] The introduction of 5 mass % DND into PSF decreases the friction coefficient against metal by 30% and leads to a threefold increase in wear resistance.[243] Small amounts of DND (0.5 mass %) improve the antifriction and antiwear properties of polyurethane rubber in water-lubricated boundary friction against steel. The load bearing capacity and maximum working contact pressure for modified PU are as large as 18 MPa, which is 60% higher than for neat PU, the elastic and strength characteristics of the material remaining almost unaltered.[264]

Double-layer metal–polymer coatings with 0.5 mass % DND reliably protect bearings and rotors of submersible pumps, as well as other parts, from the joint action of corrosion and wear, which makes it possible to retain high performance for a long time. The use of DND particles favours the increase in density and coating–substrate adhesion strength, as well as high adhesion of a lubricant to the frictional surface; as a result, the service life of parts increases by 1.5–2 times. DND-modified polymer coatings are characterized by high antifriction properties, mechanical strength, the absence of toxicity, quiet operation, good machinability by cutting tools and high resistance to liquid fuel, mineral oils and fats, organic solvents, alkalis and acids.[224, 227, 263]

In friction and wear processes, DND particles have a strong reinforcement effect on the amorphous phase of a polymer and considerably increase the hardness of the attrition face. In addition, particles that fall into the transfer film from the composite can be fixed in microheterogeneities of a counterface, decrease its roughness, and block the fraction of the surface occupied by a metal adhesively active to the polymer. As a result, the abrasivity of the counterface is reduced, which leads to a decrease in wear.

Thus, the review of recent studies dealing with design of polymer–nanodiamond composites confirms the importance and prospects of research in this area; some of the results of these studies are already worthy of industrial application.

IV. Electroconductive polymer composites

In this section, we consider hybrid nanocomposites based on conjugated polymers (CPs) and low-dimension (1D or 2D) inorganic structures: carbon nanotubes (CNTs); layered transition metal oxides (V_2O_5), oxochlorides (FeOCl) and chalcogenides (MS_2, M = Mo, Ta, Nb, W); silicates and graphite or graphene. Available methods of fabrication of nanomaterials and their structure and morphology and electrical and electrochemical properties are discussed.

1. Hybrid 1D nanocomposites of conjugated polymers and carbon nanotubes

Since the discovery of carbon nanotubes in 1991,[265] interest in them has not abated, first of all, due to a remarkable combination of their inherent properties, such as high thermal stability and mechanical strength and high electrical and thermal conductivity. The prospects of creating polymer composites containing CNTs are associated with the possible manifestation of the synergistic effect[266–268] and, as a result, with the expansion of areas of application.

Composite nanomaterials based on conductive conjugated polymers (such as polythiophene (PT), PANI, polypyrrole (PPY), and polyphenylenevinylene) and CNTs are good candidates for use in organic electronics and electrorheology, for design of microelectromechanical systems, supercapacitors, sensors and biosensors, solar cells, dis-

plays, *etc*. Among a great number of conductive polymers, PANI is the best studied and unique and most suitable for creation of composite materials owing to its easy production, stability, high electroconductivity and ease of redox processes.[269–271] Therefore, it is not surprising that the vast majority of studies on hybrid materials based on conjugated polymers and CNTs deal with PANI as the polymer component.

a. Preparation of 1D nanocomposites based on conjugated polymers and carbon nanotubes

To date, a variety of methods of fabrication of PANI/CNT nanocomposites have been developed. They imply dissolution of the polymer in a suspension of CNTs in an organic solvent,[272] melt mixing of the polymer and CNTs,[273] grafting of macromolecules to the CNT surface,[274] and electrodeposition of PANI onto CNTs.[275,276] However, the CNT propensity for aggregation gives rise to difficulties in obtaining the homogeneous fine distribution of CNTs in the polymer matrix. This is caused by insolubility of CNTs in organic solvents and incompatibility of CNTs and the polymer. A high degree of dispersion can be achieved by *in situ* polymerization of monomers in the presence of CNTs. *In situ* oxidative polymerization of aniline on multiwalled carbon nanotubes (MWNTs) affords a homogeneous polymer coating, and its thickness depends on the content of nanotubes in the reaction mixture.[277–286] The presence of MWNTs in the reaction system sharply increases the aniline oxidation rate.[287] The presence of only 1 mass % MWNTs (with respect to the monomer) reduces the polymerization time from 64 to 17 min due to the decrease in the induction period. The aniline monomer, intermediates and oligomers are adsorbed onto the MWNT surface, providing the autocatalytic growth of the polyaniline coating. Single-walled carbon nanotubes (SWNTs) have an analogous effect.

Hybrid PANI/CNT nanomaterials have also been synthesized by *in situ* emulsion polymerization.[288,289] In this case, protic acids, such as dinonylnaphthalenesulfonic acid and dodecylbenzenesulfonic acid (DBSA), simultaneously act as a dopant and emulsifier.[290,291]

The use of ultrasonication to aid both mixing and polymerization per se not only ensures a fine distribution of MWNTs in an aqueous medium but also prevents the coagulation of nanotubes in the course of emulsion polymerization.[292] The emulsion polymerization of aniline in the presence of MWNTs under common conditions without ultrasonic initiation leads to formation of agglomerates 1–4 μm in size. The use of ultrasonication only at the stage of mixing MWNTs also does not lead to their high degree of dispersion: the resulting agglomerates are 0.5–2 μm in size. The use of ultrasonication at both stages, dispersion of nanotubes and polymerization, ensures more efficient interaction of aniline with the MWNT surface.

Hybrid PANI/MWNT nanocomposite has been synthesized by the ultrasonically assisted interfacial dynamic inverse emulsion polymerization of aniline in the presence of MWNTs in chloroform.[293] Surfactant camphorsulfonic acid (CSA) was used as a dopant and ammonium peroxodisulfate (APS) served as an oxidant. The organic phase with ultrasonically dispersed MWNTs contains aniline and CSA, and the aqueous phase is a suspension of very small APS droplets. A layer of PANI is formed at the interface upon the reaction of APS radicals with the aniline–CSA complex. The resulting PANI/MWNT nanocomposites form stable suspensions in chloroform, whereas MWNT nanoparticles dispersed in chloroform that contains CSA, rapidly coagulate and precipitate.[294,295] Thus, PANI is a stabilizer of MWNT dispersion in chloroform.

As shown by scanning electron microscopy (SEM) and low-temperature TEM, the polymer (PANI) form, on the MWNT surface, a homogeneous, continuous polymer coating 10–50 nm thick. The tubes coated with PANI form networks. The suggested method enables very fast polymerization: at the ratio [aniline] : [CSA] : [APS] = 1 : 2 : 0.5, 82% conversion is achieved within 5 min of sonication. Such an effect is caused by the large interface surface area, as well as by the high concentration of APS radicals formed under sonication. It is worth noting that dynamic inverse emulsion polymerization without ultrasonic mixing and static interfacial polymerization proceed at very low rates.[296,297]

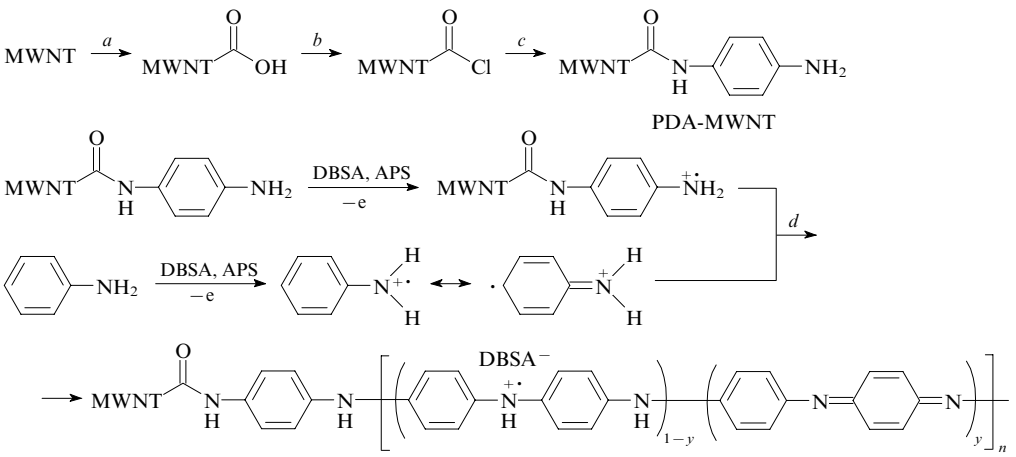
A fundamental feature of the above 1D hybrid materials is strong $\pi-\pi^*$ interaction between the quinoid units of PANI and the MWNT surface, which has been proved by electronic, IR, X-ray photoelectron and Raman laser spectroscopies. The strong $\pi-\pi^*$ interaction between the nanomaterial components is caused by that, during the *in situ* polymerization of aniline, planar quinoid units of PANI ensure formation of polymer chains in immediate proximity to the CNT surface, forming a coaxial shell on CNTs and providing charge transfer from the quinodiimine moieties of the polymer chain to CNTs.[274,281] Notwithstanding the fact that there is strong $\pi-\pi^*$ interaction between the components in the nanocomposite, this interaction is much weaker than covalent bonding. The parallel arrangement of the polymer chains and CNTs significantly increasing the interaction between the nanotubes and polymer coating has also been observed for nanomaterials based on sulfonated PANI,[298] poly(*p*-phenylenevinylene) and the copolymer of *m*-phenylenevinylene and 2,5-dioctyloxy-*p*-phenylenevinylene.[299]

In the above methods of fabrication of 1D hybrid materials by means of *in situ* polymerization in the presence of CNTs, special synthesis conditions should be met to ensure the formation of the polymer layer only on the CNT surface and prevent polymerization in the bulk, which results in a morphologically inhomogeneous material. In particular, for polymerization to occur only on the surface, the monomer concentration should be low and the ratio of the reaction volume to the surface area of the carbon substrate should be high.[300,301]

Another approach to achieve high dispersion and homogeneity of the CNT distribution implies modification of CNTs leading to the change in their surface properties. Both noncovalent surface modification and covalent functionalization are possible. Sorption of aniline oxidants — $IrCl_6^{2-}$ and 2,2′-azinobis(3-ethylbenzothiazoline-6-sulfate) (ABTS) — on the CNT surface significantly promotes the oxidative dimerization of aniline on the CNT surface to produce oligomeric intermediates responsible for the autocatalytic growth of the PANI chain.[270,302] As a result, PANI forms mainly as a homogeneous shell around CNTs, and the fraction of the free polymer considerably decreases.[303] When ABTS is used, the nanocomposite completely lacks the free PANI phase.

Polymerization in the presence of covalently functionalized CNTs not only provides the formation of a homogeneous nanostructure but also prevents the microphase

Scheme 1



separation. In particular, hybrid nanomaterials in which PANI (Refs 284 and 304), sulfonated PANI (Ref. 305) or poly(4-phenylaminobenzosulfonic acid[306] are grafted to MWNTs, as well as sulfonated PANI is grafted to SWNTs,[307] have been prepared in which the polymer forms a coaxial shell on the CNT surface.

An efficient method of synthesis of stable 1D hybrid nanomaterials in which PANI chains are grafted to MWNTs is *in situ* emulsion polymerization of aniline in the presence of covalently functionalized MWNTs. This method afforded a nanomaterial in which PANI chains are grafted to MWNTs functionalized with *p*-phenylenediamine.[308] The synthesized composite nanoparticles are multi-walled nanotubes bearing phenylenediamine (PDA) moieties and coated with a PANI layer doped with DBSA. The synthesis of these nanocomposites is shown in Scheme 1 and involves the following stages: (*a*) oxidation of MWNTs by a mixture (3 : 1) of concentrated sulfuric and nitric acids, (*b*) interaction of $SOCl_2$ with DMF, (*c*) addition of *p*-phenylenediamine in a nitrogen atmosphere, and (*d*) preparation of a micellar dispersion of functionalized MWNTs (PDA-MWNTs) in DBSA, addition of aniline and an aqueous solution of an oxidant — APS (the ratio [DBSA] : [$PhNH_2$] : [APS] = 0.8 : 1 : 1). The *in situ* polymerization occurs at 30 °C. It is essential that all stages occur under ultrasonication.

IR and Raman spectroscopy has proved that DBSA-PANI chains are covalently bonded to functionalized MWNTs through amide groups.

b. Electrical properties of 1D PANI/CNT composites

Strong $\pi-\pi^*$ interaction between quinoid units of PANI and six-membered rings of the graphene surface of CNTs promotes electron transport in a nanomaterial as compared with the neat polymer, thus improving the macroscopic conductivity parameters. The surface resistance of the PANI/SWNT nanocomposite film on an SiO_2 plate is 16.9 kΩ/□, which is one order of magnitude lower than the resistance of PANI (343.3 kΩ/□) and MWNTs (222.7 kΩ/□).[293]

Ultrasonic treatment has a considerable effect on the conductivity parameters of nanocomposites. The conductivity of PANI/MWNT produced under sonication at all stages of synthesis of the hybrid nanomaterials is 27 S cm^{-1}, which significantly exceeds the conductivity of PANI/MWNT nanocomposites obtained with the use of sonication only for mixing (2.5 S cm^{-1}) and under common conditions of emulsion polymerization (4.6 S cm^{-1}).[292] An increase in conductivity is explained by the ultrasonically induced increase in the donor–acceptor interaction between the quinoid units of PANI (strong donor) and MWNTs (strong acceptor). It has been shown that, with an increase in ultrasonic treatment duration, the surface resistance increases as a result of gradual conversion of the conducting PANI form into the nonconducting form of the emeraldine base.[309]

The electroconductivity of the DBSA–PANI/PDA–MWNT nanocomposite[308] at room temperature (13.65 S cm^{-1} after polymerization for 3 h) is at least an order of magnitude higher than the conductivity of PANI doped with DBSA (1.03×10^{-2} S cm^{-1}). The high conductivity of the samples produced within 3 h of polymerization is due to the ordered structure and the high content of functionalized MWNTs. The phenylenediamine moieties grafted to the MWNT surface act as bridges, promoting electron density delocalization, which enhances charge transport. As a result, the conductivity of the hybrid nanomaterials increases at least by an order of magnitude as compared with that of PANI doped with DBSA.

With an increase in the polymerization duration to 6 h, the content of functionalized MWNTs is reduced, and according to X-ray diffraction data, the upper (near-surface) layers of the PANI coating have a disordered structure with a high content of amorphous regions so that the conductivity decreases to 0.623 S cm^{-1}.

Noteworthy is the fact that ultrasonication in the course of polymerization leads to the 'cutting' of MWNTs. Nanostructures obtained by polymerization for 3 h are 1–3 μm in length and 100 nm in diameter (the aspect ratio is 10–30). With an increase in the reaction time to 6 h, the length of most of nanostructures decreases to 0.3–1.5 μm, the average diameter being 120 nm (the aspect ratio is 2.5–12.5). The decrease in nanoparticle size has an effect on charge transport in the nanocomposite so that the conductivity is reduced.

The 1D nanomaterials considered in this section have high potential for use as electrode materials for electrochemical power sources, electrolytic capacitors, sensors, *etc.* Therefore, it is vital to scrutinize their electrochemical behaviour. Comparison by cyclic voltammetry of the electrochemical properties of the PANI, PANI/MWNT and PANI/MWNT modified with $IrCl_6^{2-}$ and ABTS (Ref. 303) has shown that the electrochemical properties of the nanocomposites are determined by the redox transitions of

PANI. Of crucial importance is that the potential difference between the anodic and cathodic peaks ($\Delta E = E_a - E_c$) decreases, which corresponds to the increase in reversibility of electrode reactions. Most likely, this is associated with an increase in the charge transfer rate in the MWNT–PANI system as compared with neat PANI.

Studying electrochemical capacity retention in composites upon long-term cycling has demonstrated the high stability of composites with modified MWNTs during charge/discharge processes. After 100 thousand cycles, their losses were only 5%–6% of the starting value, whereas the losses of composites with unmodified MWNTs were as large as 20%.

Thus, in the past decade, efficient methods of fabrication of hybrid 1D nanomaterials based on conjugated polymers and CNTs have been developed. The polymer forms a coaxial shell on the CNT. This shell can be covalently bonded to the CNT surface or be held by strong $\pi-\pi^*$ interaction between the components of nanomaterial. The introduction of CNTs into a nanomaterial increases its thermal stability and ensures the increase in electroconductivity owing to stronger electron density delocalization and, as a result, enhancement of electron transport in the system.

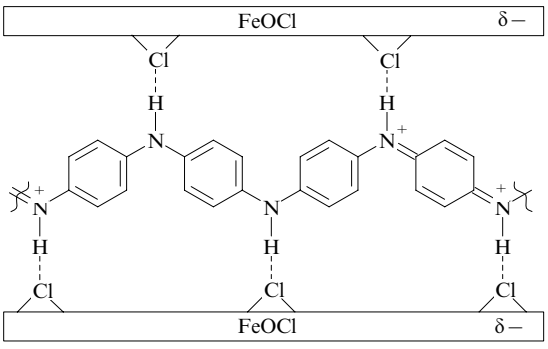
2. Hybrid 2D nanocomposites based on conjugated polymers

A methodology of synthesis of 2D hybrid nanomaterials is based on intercalation of conductive conjugated polymers into layered inorganic structures [310] and is dictated by the nature of both the layered material ('host') and the intercalated polymer ('guest'). Transition metal oxides and oxochlorides (FeOCl, V_2O_5 xerogel), metal chalcogenides (MeS_2, Me = Mo, Nb, Ta and others), layered silicates (MMT, smectite, hectorite) and graphite are used as two-dimensional layered materials.

a. Nanocomposites based on conjugated polymers and metal oxides and oxochlorides

Kanatzidis *et al.*[311] were the first who applied *in situ* polymerization of pyrrole to produce the hybrid nanomaterial PPY–FeOCl. The method involves the introduction of monomer molecules into the interlayer space of FeOCl followed by oxidative polymerization. In addition to PPY, PANI and PT have been intercalated into the FeOCl lattice.[312–316] Formation of hydrogen bonds between NH groups of the monomer and Cl atoms of host has been revealed. The PANI bonding in the FeOCl structure is shown in Scheme 2.[317] As follows from spectral data, the resulting polymers are in the conducting form, which determines the electrical properties of the synthesized nanomaterials.[311,318]

Scheme 2



In synthesis of hybrid materials by intercalation of conducting polymer into the interlayer space of FeOCl, V_2O_5 and $VOPO_4$, it is crucial that the layered inorganic compounds themselves initiate oxidative polymerization, simultaneously acting as dopants. *In situ* oxidative intercalation polymerization of aniline, pyrrole and bithiophene in the interlayer galleries of the V_2O_5 xerogel affords nanomaterials with a structure of alternating layers of the electroactive polymer and vanadium oxide.[317,319–322] The synthesis conditions have a strong effect on the mechanism of formation of a nanomaterial and its morphology. In particular, intercalation polymerization of aniline in V_2O_5 in an aqueous medium in the presence of HCl at 120 °C leads to formation of composite nanosheets.[323] At the early stages in an acid medium (pH 3), the anilinium cation diffuses into the intersheet galleries of V_2O_5, where oxidative polymerization occurs. At further stages of polymerization yielding intercalated PANI, V_2O_5 is exfoliated to give 10–20 nm thick nanosheets, which self-assemble into supramolecular nanostructures (Fig. 6); this is accompanied by partial reduction of V^{5+} to V^{4+}. At room temperature, nanosheets are not formed, and the resulting hybrid material has a rod-like morphology. In the absence of an acid, sonochemically initiated polymerization of aniline in the interlayer space of V_2O_5 leads to a nanomaterial in the form of nanowires.[324]

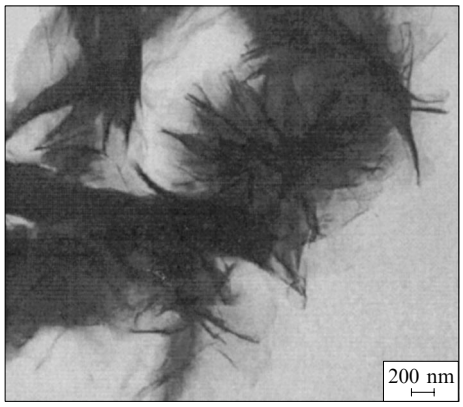


Figure 6. TEM image of the PANI–V_2O_5 nanocomposite ([$PhNH_2$] = 0.016 mol litre^{-1}, 120 °C, 24 h).[323]

The process of preparation of a hybrid nanomaterial and its morphology are radically different when intercalation polymerization is carried out under homogeneous conditions of the reaction between aniline and peroxyvanadic acid, which forms upon dissolution of V_2O_5 in an aqueous solution of hydrogen peroxide.[325,326] The product is a hybrid material with a hierarchical morphology composed of differently oriented nanoplates and nanostrips.[327] Figure 7 shows the SEM image of such a structure. According to X-ray diffraction, the end product has a lamellar structure with intercalated PANI chains.[310,316,328] The interlayer distance for the (001) reflection peak is 13.6 Å and remains constant with an increase in polymerization duration, which is consistent with the results [319,321]. The morphology of the hybrid nanomaterial depends on synthesis temperature and duration. At room temperature, no polymerization occurs, and a hybrid material does not

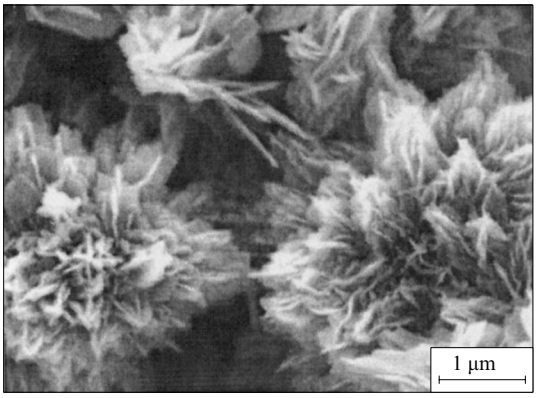


Figure 7. SEM image of the hierarchical nanostructure of the hybrid nanomaterial PANI – V_2O_5 obtained at 180 °C in 24 h.[327]

form. At 80, 120 and 180 °C, polymerization leads to nanostrips, nanoplates and nanosheets, respectively. As shown by X-ray diffraction and IR spectroscopy, the galleries accommodate PANI chains and water molecules. Simultaneously, vanadium is reduced to V^{4+}. At 180 °C, with an increase in polymerization time to 4 h, aniline continues reacting with peroxyvanadic acid to give a hybrid nanostructure resembling flowers composed of arbitrarily oriented 20 – 30 nm thick nanoplates and with horizontal dimensions of 1 – 2 μm. The hybrid material formed within 24 h has a supramolecular structure with a hierarchical morphology and close-packed nanoplates. As the process develops, water molecules leave the V_2O_5 galleries.

The PANI – V_2O_5 nanocomposites are electroactive in aqueous acids and aprotic electrolytes.[329] Cycling of the nanomaterial in 1 M HCl in the potential range from −0.2 to 1.0 V does not lead to its degradation. The cyclic voltammogram show one broad peak, whereas two peaks are observed for neat PANI under the same conditions. The electrochemical activity of nanocomposites is associated with electron transfer between the redox sites of nanocomposite components. Direct charge-transfer interaction between the macromolecules intercalated into the intersheet galleries of V_2O_5 and V^{5+} giving rise to a joint electronic system has been demonstrated by EPR spectroscopy. Electron transfer from the lone pair of the nitrogen atom of PANI to V^{5+} is identified in the EPR spectra, which show the signals of PANI paramagnetic centres ($g = 2.0023$) and V^{4+} ion ($g = 1.967$). Thus, the obtained PANI – V_2O_5 nanomaterials are of interest as stable electrode material with a wide range of electrochemical activity.

b. Nanocomposites based on conjugated polymers and metal chalcogenides

Consider formation of hybrid nanomaterials based on conjugated polymers and transition metal chalcogenides for conducting polymers and MoS_2 as an example. A characteristic feature of the layered chalcogenide MoS_2 is that it has a sandwich S – Mo – S structure where a layer of Mo atoms is located between two layers of S atoms, and each Mo atom in the layer is coordinated to six S atoms. The sandwich layers owing to the S – Mo bonds have a trigonal prismatic or octahedral configuration and are bound to each other through van der Waals interactions.[20]

At the first stage, formation of a hybrid layered nanomaterial based on a conducting polymer and MoS_2 involves exfoliation of MoS_2 and formation of a colloid suspension. The scheme of the process is shown in Fig. 8. The reaction of MoS_2 and Bu^nLi in hexane yields the intercalated compound Li_xMoS_2:

$$MoS_2 + Bu^nLi \longrightarrow Li_xMoS_2 + 0.5\,C_8H_{18}$$

The x value depends on reaction temperature and is 1.12 at 80 °C. Under ultrasonic mixing in an aqueous medium, Li_xMoS_2 is subjected to exfoliation to form a colloid dispersion:

$$Li_xMoS_2 + H_2O \longrightarrow (MoS_2)_{monolayers} + LiOH + 0.5x\,H_2$$

Complete exfoliation is observed at $x > 0.9$. After neutralization, the suspension is stable for several days.

Then, two approaches are possible. The first one is direct introduction of the polymer into the layered structure of MoS_2 . The polymer (PANI or its alkyl derivatives, PPY) is first dispersed in water or organic solvent and then added to exfoliated MoS_2 and stirred at room temperature for 4 h.[331 – 336]

$$(MoS_2)_{monolayers} + x\ \text{polymer} \longrightarrow (\text{polymer})_x - MoS_2$$

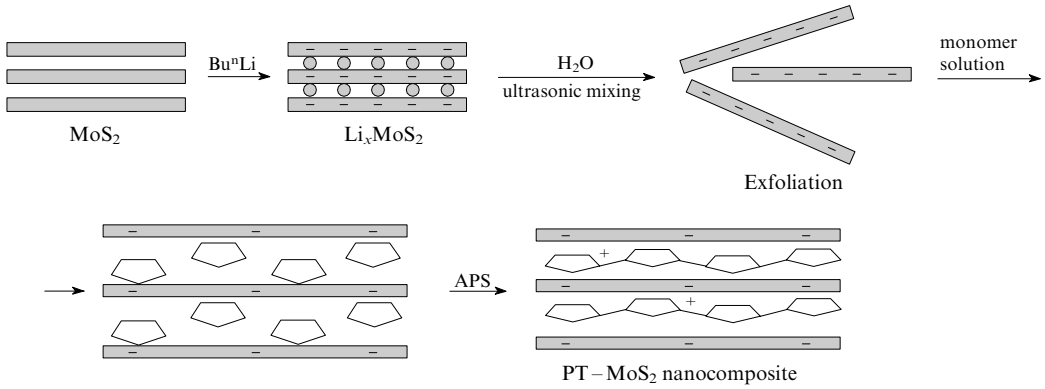


Figure 8. Scheme of synthesis of the PT – MoS_2 nanocomposite.[330]

The other synthetic route implies the introduction of the monomer into a colloid suspension of exfoliated MoS_2 with subsequent oxidative polymerization in the intersheet galleries of the host. This approach has been used for intercalation of PANI, PPY and PT into the intersheet galleries of MoS_2.[330, 337–339] The monomer introduced into the colloid system is adsorbed onto the surface of exfoliated MoS_2 monolayers. Subsequent oxidative polymerization leads to the polymer intercalated between the MoS_2 layers. It is worth noting that the oxidant (APS) modifies not only the monomer but also the resulting polymer (p-doping) so that the latter becomes positively charged. Since the MoS_2 layers have partial negative charge owing to the presence of electronegative sulfur atoms,[338] there is electrostatic interaction between the host layers and the guest, the p-doped polymer, which is responsible for flocculation of the intercalated polymer.

According to X-ray diffraction, the intercalation of PPY, PT and PANI and its alkyl derivatives increases the interlayer spacing of MoS_2 by 3.5–5.4 Å.[331, 332, 334, 337, 339] This is evidence that the polymer forms monolayers in the intersheet galleries of the host, and the macromolecules tend to align parallel to the MoS_2 layers. It has been demonstrated for the PPY–MoS_2 nanocomposite[339] that, depending on the synthesis conditions, the orientation of polymer chains can be changed. When polymer chains are parallel to the host layers, the planes of heterocyclic rings of the PPY chains are parallel to the MoS_2 layers, which is favoured by strong interaction between the π-orbitals of the guest heterocycles and the electronegative sulfur atoms of the host. If the polymer chains are perpendicular to the host layers, the planes of the heterocycles of PPY are also perpendicular to the host layers, and interaction between the polymer chains and MoS_2 is completely absent.

Owing to the interaction of the conjugates system of the guest with semiconductive layers of the host, the conductivity of the nanocomposites is higher than that of corresponding neat polymers and MoS_2. The increase in conductivity is due to the fact that the presence of the polymer monolayers in the galleries facilitates electron transport between the organic and inorganic components of the nanocomposite. In addition, MoS_2 can rearrange from the trigonal prismatic (semiconductive) structure into the octahedral (metal-like) structure.[340–342] The presence of even a small amount of metal-like MoS_2 also contributes to the increase in conductivity.

The conductivity of intercalated nanocomposites depends on the conformation and stereoregularity of conducting macromolecules in the MoS_2 galleries.[339] At 10 °C, higher conductivity is exhibited by the nanocomposites in which the PPY heterocycles are parallel to the MoS_2 planes and, thus, promote electron transport between the organic and inorganic components of the nanocomposite. If the planes of the polymer molecules are perpendicular to the host planes, the interaction between the π-system of PPY and MoS_2 is absent, and the nanocomposite conductivity is determined only by the PPY conductivity since the MoS_2 conductivity is significantly lower.[343] At 0 °C, the conductivities of nanocomposites of both types are the same, remaining higher than the conductivity of neat PPY. This is explained by topochemical polymerization of pyrrole between the MoS_2 layers, which occurs in the temperature range from −60 to 10 °C and leads to formation of a stereoregular polymer, whereas bulk polymerization yields atactic PPY. At −60 °C, the conductivity of neat PPY and the composites is the same and decreases with a further decrease in temperature since, at low temperature, it is determined only by the charge carrier concentration.

c. Nanocomposites based on conjugated polymers and layered silicates

Layered silicates, especially Na^+-MMT, are used for fabrication of conducting polymer nanocomposites by means of introducing conjugated polymers into clay galleries by different methods.[68, 344–350]

Most frequently, intercalation of conjugated polymers into the silicate structure is carried out by exchanging the cations in the galleries for transition metal cations, which act as polymerization catalysts. A monomer adsorbed in Cu^{2+}-MMT is oxidized to form radical cations, initiating the growth of a polymer chain. The Cu^{2+} ion is thereby reduced to the Cu^+ ion, which rapidly disproportionates to give the polymerization catalyst Cu^{2+} (Ref. 344). The proposed method has been used for introduction of PANI, PPY, poly(*p*-phenylene), PT and polymethylthiophene into the intersheet galleries of MMT, smectite and fluorohectorite. This gives rise to a monolayer packing of polymer chains, and their heterocyclic or aromatic rings are parallel to the silicate planes.[344] To intercalate PPY into MMT galleries, inverse emulsion polymerization was used, with DBSA as a emulsifier and dopant and APS as an oxidant.[350] It has been shown that the NH groups of PPY and surface oxygen atoms of MMT are hydrogen bonded.[349]

The second route is the introduction of colloid nanoparticles of polymers into a dispersion of MMT exfoliated in water. This method does not require the presence of transition metal ions for initiation of polymerization and produced the hybrid nanomaterial based on PT and MMT without introduction of oxidants.[345] Thiophene is known to polymerize very slowly in the presence of strong Lewis acids ($FeCl_3$) because of its higher oxidation potential as compared with pyrrole and aniline.[351] At the same time, it polymerizes in high yield in the bulk and in a solution in chloroform at the thiophene boiling temperature in the presence of MMT without introduction of oxidants. It is suggested that polymerization yielding PT between MMT layers is initiated by the thiophene radical cation generated by electron transfer in the monomer complex with cations in MMT galleries.

The third route for creating nanocomposites is to exchange Na^+ ions in MMT for the anilinium cation in MMT by keeping clay on a solution in aqueous HCl with subsequent polymerization in the presence of chemical oxidant,[344] electrochemically[352] or mechanochemically.[353, 354] To increase the content of polymer chains in MMT galleries, the Na^+ cations were completely replaced by protons, and the protonated MMT was treated at 80 °C with a 0.4 M solution of HCl containing a 10-fold excess of aniline, or in the absence of an acid, anilinium cations were introduced into intersheet galleries of protonated MMT.[355] Intercalation polymerization was carried out by adding a APS solution in 0.1 M HCl to a suspension of protonated aluminosilicate preliminarily saturated with the monomer. Polymerization was carried out at 0–2 °C for 8 h under permanent stirring.

A maximal content of aniline (20 mass %) in the MMT galleries has been achieved by means of borderline polymer-

ization.[300, 301, 356, 357] In this case, PANI is formed as monolayers in galleries and on the surface of clay particles.

Conducting polymer/clay materials have an electronic type of conductivity. The conductivity of nanocomposites is always lower than the conductivity of the polymer filling the intersheet galleries. The conductivity magnitude is determined by the concentration ratio of the conjugated polymer and MMT and varies within the range 2.0×10^{-5}–1.5 S cm^{-1} (Refs 345, 349, 358–366). Clearly pronounced anisotropy of the conductivity of the PANI/fluorohectorite and PPY/smectite layered nanocomposites has been revealed.[366, 367] The conductivity anisotropy coefficient was $\sim10^5$ in the first case and 4.0×10^3, in the second case.

For creation of dominant orientation of clay particles, a pressing method has been used.[355] In the bulk of material, a state is generated that is characterized by shear and normal strains, which are favourable for orientation of planar particles along the shear direction. The resulting ordering of PANI/MMT particles provides efficient transport of charge carriers from particle to particle in the direction of preferred orientation.

As already mentioned, the borderline polymerization method[300, 357] makes it possible to increase the polymer content in the nanocomposite owing to formation of the conjugated polymer not only in clay galleries but also on the surface of silicate sheets. In-plane compression leads to predominantly planar ordering of anisodiametric clay particles with an adsorbed or intercalated polymer. As a result, a nanomaterial with conductivity anisotropy is formed, the anisotropy coefficient being as large as 6×10^3 (Ref. 355).

This class of hybrid nanomaterials exhibits excellent electrochemical properties. In particular, for electrodes based on the PPY/MMT nanocomposite, the working range of potentials increases by 1 V.[368] Such electrodes are more stable than electrodes based only on clay or only on PPY.

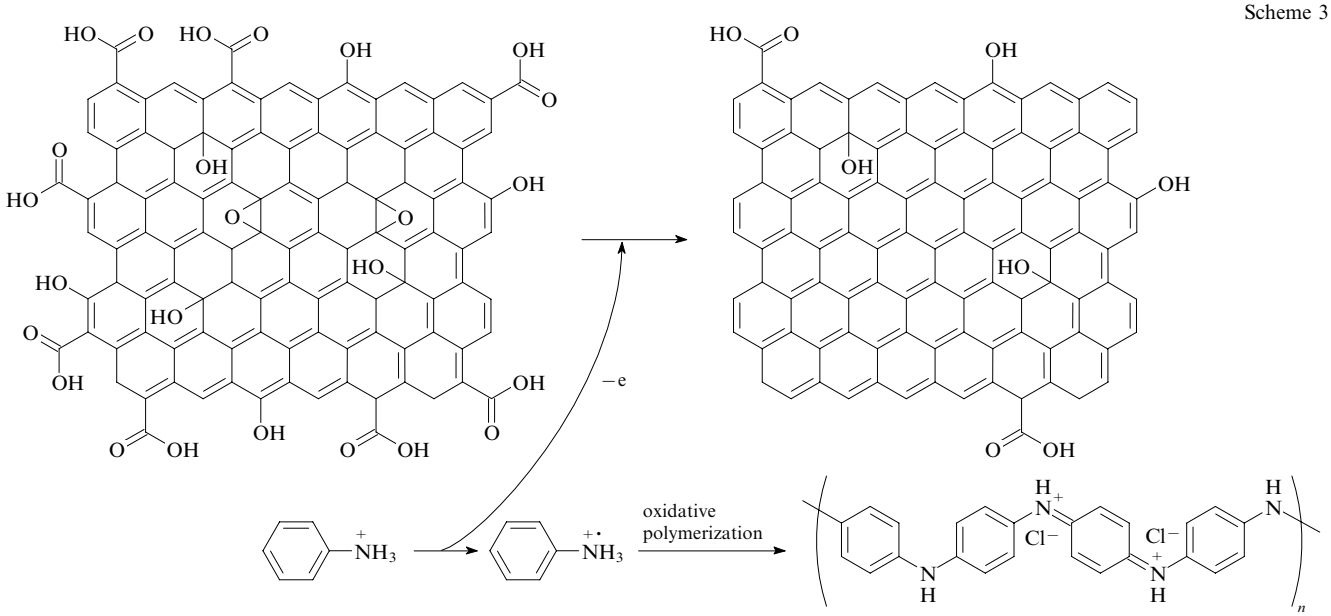
d. Nanocomposites based on conjugated polymers and graphene structures

Graphene, a one-carbon-atom thick sheet with atoms arranged in a regular hexagonal pattern, has unique electrical, optical, catalytic and mechanical properties so that its synthesis has attracted considerable interest of researchers.[369–372] Like graphene, graphene oxide (GO), obtained by exfoliation of graphite oxide, has a single-layer structure with oxygen groups in the basal planes and at the edges.[373] Two methods of synthesis of PANI/GO nanocomposites are known: mixing PANI with GO[374, 375] and *in situ* polymerization of aniline.[376, 377] Nanocomposites of PANI and reduced GO have been synthesized in one stage by combining the reactions of oxidative polymerization of aniline and GO reduction with aniline[378] (Scheme 3). Polymerization occurs at 70 °C in 1 M HCl. The reduction of GO has been proved by X-ray diffraction. With an increase in duration of reduction with aniline, a sharp diffraction peak of GO (d = 7.89 Å, 2θ = 11.2°) rapidly decreases and a new broad, strong reflection peak of reduced GO appears (d = 3.53 Å, 2θ = 25.4°);[379] the position of this peak is very close to the reflection peak of graphite (d = 3.35 Å, 2θ = 26.6°).[380]

The morphology of the nanocomposite essentially differs from that of the initial GO. GO has a lamellar morphology, whereas, in the nanocomposite, PANI fibres with a large aspect ratio arranged into spindle-like structures are located between nanosheets of reduced GO.

Graphite is a layered material with high conductivity (10^4 S cm^{-1}) at room temperature. Its structure is represented by a great number of graphene layers stacked together in which carbon atoms are arranged in a hexagonal network.[21] To synthesize a nanocomposite with graphite, the polymer should be intercalated into pores of interlayer space of exfoliated graphite nanosheets.[381–383] The procedure of preparation of the latter involves three stages: 1) intercalation of acids (H_2SO_4 and HNO_3, 4 : 1) and washing with water to neutral reaction; 2) thermal expansion at 1000–1050 °C for 15–30 s; 3) exfoliation in an ultrasonic bath. The *in situ* polymerization of aniline in the presence of exfoliated 20–50 nm thick graphite nanosheets leads to formation of the hybrid PANI/graphite nanomaterial.[384, 385] Depending in the conditions of preparation of nanosheets, the synthesis yields the composites in which

Scheme 3



either PANI is located between graphite nanosheets or these nanosheets are finely distributed in the PANI matrix.

Testing the resulting nanocomposites as the electrode material for capacitive devices by cyclic voltammetry, galvanostatic method and electrochemical impedance spectroscopy has demonstrated that the composite systems have better electrochemical performance than PANI, reduced GO and graphite nanosheets, which opens prospects for their use in capacitive energy storage systems.

Study of electrochemical properties by cyclic voltammetry has shown an increase in the conductivity of nanocomposites as compared with neat PANI.[384, 386] It is possible that graphite nanoparticles act as electron conductors and connect PANI chains, thus increasing conductivity. The conductivity of the nanocomposite achieves a maximum value of 0.67 S cm^{-1} at the 3% content of graphite nanosheets.[386]

As shown by galvanostatic charge/discharge measurements, the discharge time of the PANI/graphite nanocomposite is significantly longer than that of pure graphite nanosheets: for the latter, the time it takes for 20 cycles to pass is 38 s, while for the nanocomposite this time is 700 s.[384] Since the discharge time is in direct dependence on specific capacity, the capacity of the nanocomposite is considerably higher than that of graphite. The specific capacity of reduced GO, PANI and the nanocomposite based thereon is, respectively, 41, 115 and 286 F g^{-1}, which demonstrates enhancement of the electrochemical performance of the hybrid material.

Thus, recent interest in hybrid nanomaterials containing conjugated polymers stems from the fact that, owing to electronic interaction of the organic and inorganic components, they can exhibit excellent electrical and electrochemical properties. This circumstance makes them promising materials for use in organic electronics and in design of rechargeable batteries, sensors, supercapacitors, electrocatalysts and other electrochemical devices.

For example, the use of hybrid fibres based on PANI and CNTs (only 0.25 mass %) as the electrode material will make it possible to enhance the redox reversibility, decrease the discharge potential and increase the charging potential of electrochemical systems.[387] Aniline polymerization on the surface of carbon paper (based on graphite of graphene oxide) affords a material that combines flexibility, high electrochemical performance and biocompatibility, which makes it a good candidate for use in flexible bio-electrodes of power cells and sensors, as well as a platform for cell cultures.[388]

In addition, the above hybrid materials are distinguished by high thermal and chemical stability, which enables their operation at elevated temperatures and in corrosive environments.

V. Nanocomposites based on liquid-crystalline polymers

Among nanocomposites, a special place is occupied by the systems constituting the basis of modern materials for photovoltaics, optoelectronics, information storage systems, *etc*. They are fabricated by filling polymers with nanoparticles of noble metals or semiconductors 1–20 nm in size, in which strong spatial localization of valence electrons leads to the appearance of properties other than those of both the solid and the isolated molecules. Particles no more than 10 nm in size are most promising for realization of quantum-size effects.[389–395] Although the first important stage is the synthesis of homogeneous uncoagulated solid particles with the diameter smaller than the Bohr radius of the exciton of the bulk material, of crucial importance is the second stage involving fabrication of functional materials based on nanoparticles. One of the key issues for solving many applied problems consists not only in simple filling of the matrix but also in finding ways for controlled and accurate organization of arrays of nanoparticles. Ordered arrays formed by metal nanoparticles, semiconductor islands or quantum dots are suitable for use in the development of new optical devices, nanosensors, computers, memory systems and other systems for information processing and storage.

One of the most interesting findings of the last decade is the use of LC media as matrices that promote self-organization of nanoparticles of different shape. At the fundamental level, almost nothing is known about the effect of anisotropic environment on the physical properties of nanoparticles, and there is no appropriate molecular theory describing the optical properties of nanoparticles in an anisotropic medium, which is necessary for developing new materials and studying new effects. Nevertheless, theoretical consideration of the interaction of nonmagnetic and magnetic nanoparticles with LC director[396] has demonstrated that since the director field depends essentially on boundary conditions, the character of chemical bonding of LC phase molecules with the nanoparticle surface determines the orientation of these molecules. Consideration of two nanoparticles placed into an LC medium has demonstrated that there is long-range interaction between them. This is caused by the disturbance of the director field induced by one particle, which has an effect on the director field of the other particle. This is responsible for a specific interaction between the nanoparticles at distances equal to several nanoparticle diameters. The behaviour of nanoparticles in an LC medium is described by the magnitude of their effective charge. The spinor character of the latter determines the most energetically favourable mutual orientation of nanoparticles. First experimental studies of compatibility of nanoparticles and lyotropic liquid crystals have shown that the anisotropic matrix is responsible for a mean orientation of magnetic particles, which persists even in zero magnetic field.[397–400] The magnetic moments of particles are preferentially aligned in the plane of the ferrosmectic layers for the lamellar phase and along the axes of ferrohexagonal cylinders in the cylindrical phase. Thus, lyotropic liquid crystals are able not only to fix the positions of particles but also to have an effect on the orientation of their magnetic moments.

The chemical interaction of the molecules of a thermotropic liquid crystal with gold nanoparticles resulting in formation of an Au–S bond with retention of the LC properties of such composite materials have been described.[401–403] It has been demonstrated that the introduction of noble metal nanoparticles into an electrooptical LC matrix makes it possible to control light scattering and, as a result, induce a spectral shift of the particle plasmon resonance by applying an electric field.[404] Moreover, light scattering experiments show that spherically shaped nanoparticles become optically spheroidal when placed in an anisotropic liquid crystal. The introduction of CNTs into liquid crystals can enhance the LC order and increase the

isotropic–nematic phase transition temperature.[405] The same effect has been revealed in a liquid crystal doped with gold nanorods covalently functionalized with organic molecules resembling the molecules of liquid crystals.[406] In addition, a significant decrease in the threshold voltage for the Fréedericksz transition has been observed.[407–409] Considerable progress in control of electrooptical properties of liquid crystals used for creation of displays has been achieved in recent years by doping them with nanoparticles.[410–413]

A crucial result has been reported,[414] the authors show that the interaction of colloid particles and their self-assembly in a nematic medium can be controlled by varying the shape of nanoparticles. For polygonal crystals, it has been demonstrated that nanoparticles disturb the homogeneity of their environment, which leads to a change in the characteristics of order and directed pairwise interactions in the equilibrium state. Forces of interaction between particles have either dipole or quadrupole symmetry, depending on the set of polygon planes, which contributes to different packing of nanocrystals. In addition, it has been demonstrated that nanospherical gold particles coated with polyvinylpyrrolidone in smectic layers of liquid crystals exhibit enhanced colloid stability. Gold nanorods are capable of self-alignment in liquid crystalline phases with subsequent realignment in electric and magnetic fields.[415] Noteworthy is also the process of self-organization of gold nanorods to adopt the helical configuration of the cholesteric liquid crystalline phase.[416]

One of the important approaches developed in recent years is immobilization of nanoparticles by block copolymers.[417–427] For example, the introduction of gold, silver, indium and lead nanoparticles as the inorganic phase into the PS-PMMA block copolymer leads to formation of a lamellar structure, the nanoparticles (in particular, gold nanoparticles) being located mainly in the PS domains owing to preferential interaction. When 30 mass % of gold nanoparticles are introduced, the PS domains become electroconductive, thus converting into nanowires. The same diblock copolymer of composition at which PMMA blocks form cylindrical micelles 15–20 nm in diameter has been used as a template for self-assembly of CdSe nanoparticles. When a copolymer film is placed into a dilute solution of nanoparticles, the latter penetrates into cylindrical structures due to capillary forces. Electron microscopy showed that about 70% of cylinders are filled with nanoparticles that retain their ability to luminescence under self-assembly conditions with subsequent acidic etching of the substrate, and the luminescence intensity can be controlled by varying the concentration of nanoparticles in solution. The structure of similar composites is determined by the size and shape of nanoparticles.

Three-dimensional assemblies of metal nanoparticles are of great interest as plasmonic materials. Their properties essentially depend on the type of metal and particle size and shape, as well as on the character of their self-assembly. Microphase separation in block copolymers is favourable for creation of nanosized periodic structures in which the particles are self-assembled to fit the type of domain structure of the polymer matrix, which has an effect on the plasmonic properties of the system as a whole.[428]

In parallel with experimental studies of block copolymer/nanoparticles composites, the self-consistent field theory has been developed to describe the effect of nanoparticles on phase separation in diblock copolymers.[425, 429, 430] Calculations showed that, depending on the selected key parameters, namely, the particle size, block chain lengths and parameters of interaction between nanoparticles and different blocks with each other, nanoparticles can be located either at the centre or at the edges of lamellar or spherical domains. Later,[431] a theoretical approach has been suggested that is based on a field-theoretic description of the polymer melt in which the coordinates of impermeable particles are specified explicitly. The role of nanoparticle size, as well as of the concentration and composition of copolymers has been experimentally demonstrated for gold and FePt nanoparticles in composites based on PS–PEO block copolymers.[432, 433]

Functionalization of gold nanoparticles with ligands containing groups capable of molecular recognition enables their assembly inside polymer scaffolds.[434–436] With the use of anisotropic gold nanorods, filled anisotropic PVA films have been fabricated in which particles are aligned by stretching the matrix above glass transition temperature with subsequent cooling to fix the alignment.[437] Yet another interesting approach has been suggested for fabrication of LC phases based on different rod-like nanoparticles functionalized with PMMA, PS and PEG macromolecules.[438–440] In this case, nanorods dispersed in organic solvents or PEG and PS oligomers self-assemble to form LC phases.

At the Topchiev Institute of Petrochemical Synthesis, Russian Academy of Sciences, a new approach have been suggested and realized for design of functional nanocomposites with controlled localization and distribution of nanoparticles in the bulk of matrices based on comb-like LC polymers. The approach is based on the consideration of four major factors: the chemical structure of a polymer, the

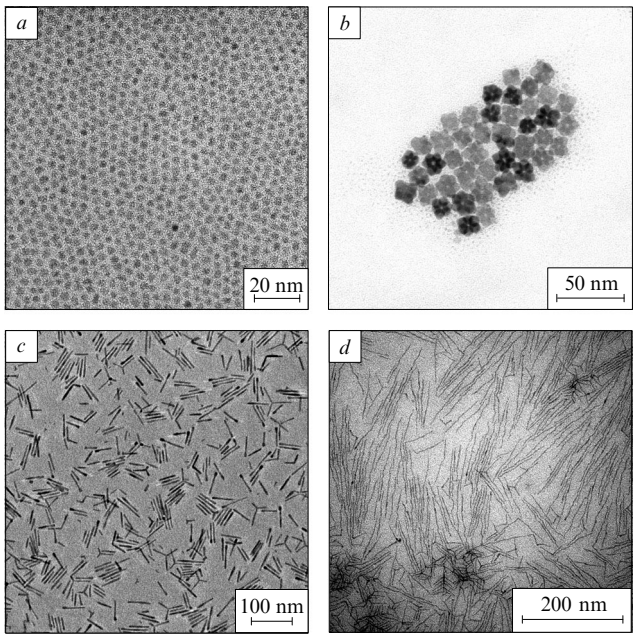


Figure 9. Nanoparticles of (*a*) CdSe, (*b*) PbSe and (*c*, *d*) CdS semiconductors synthesized at the Topchiev Institute of Petrochemical Synthesis, RAS.

structure of an LC phase, the type of interaction responsible for its formation and, finally, the possibility of chemical bonding of the matrix with the nanoparticle surface.

It is evident that, from the viewpoint of nanoparticle shape, nanorods and nanodiscs have better chance to undergo LC matrix-assisted assembly. Figure 9 shows semiconductor nanoparticles some of which have been used in investigations described below, namely, spherical nanoparticles (quantum dots), polygonal nanocrystals, nanorods and nanowires.

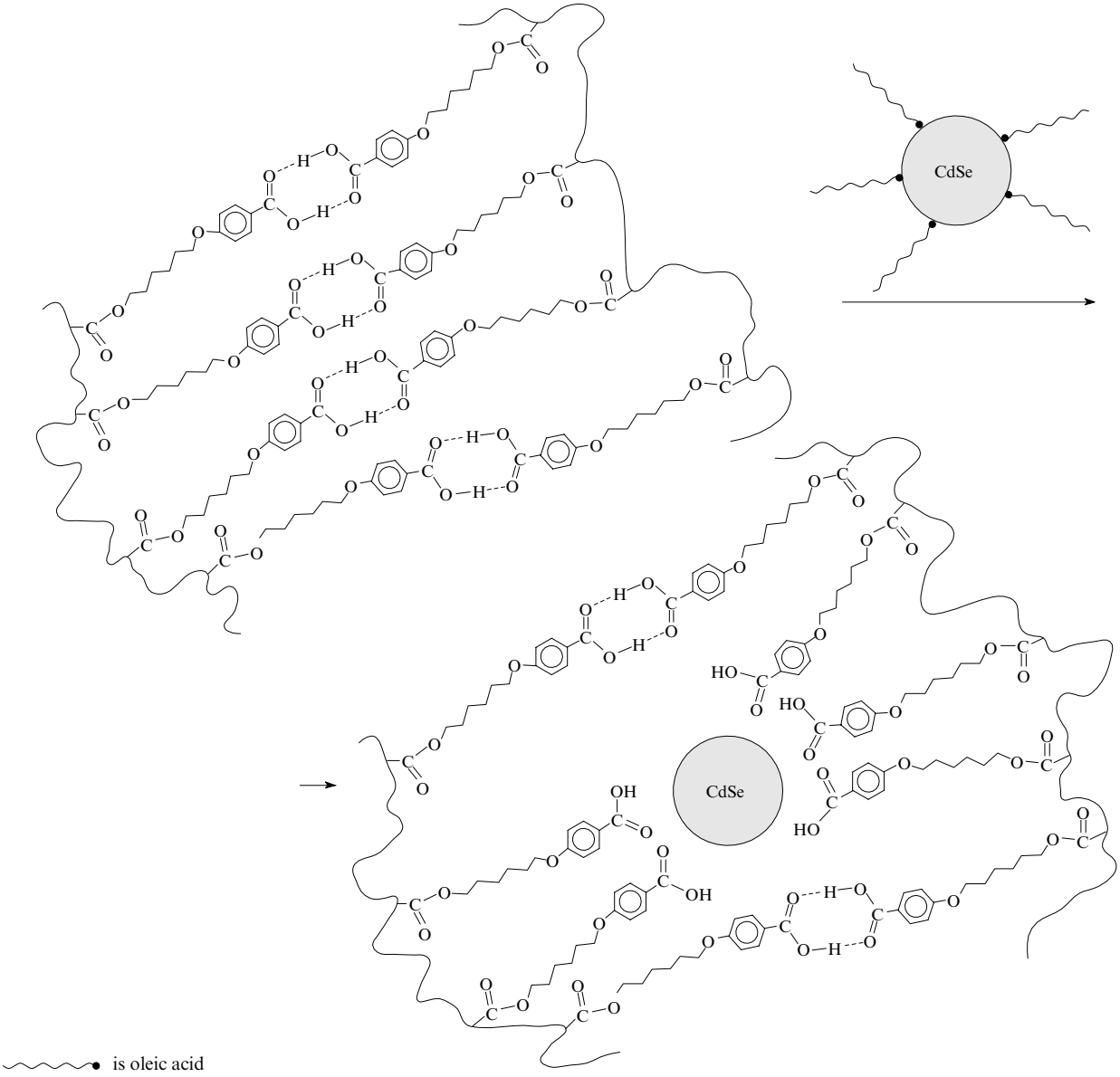
As polymer matrices, polymers based on 4-(ω-acryloyloxy)alkoxybenzoic acids (BA-*n*PA) with polymethylene pendant chains of different length (*n*) were used. These polymers completely meet the requirements for the use of polymer matrices in the new approach. The polymers form a tilted smectic C phase.[441]

Macromolecules contain moieties with functional carboxyl groups. The latter form dimers responsible for formation of mesogenic fragments through hydrogen bonding and, as a result, promote the formation of the LC phase.[441, 442] In addition, the presence of functional groups implies their possible interaction with the nanoparticle surface.

Scheme 4 shows the schematic of the possible mechanism of controlled introduction of nanoparticles into the matrix of LC polymers of the BA-*n*PA type. It is well known that nanoparticles can be stabilized in organic solvents if their surface is covered with various hydrophobic molecules. In this case, we are talking about CdSe quantum dots stabilized by oleic acid molecules,[443, 444] or about CdS nanorods modified with trioctylphosphine oxide (TOPO) molecules and synthesized by a published procedure.[445] It has been assumed that if the composite preparation method[446] is properly selected, the macromolecules containing functional groups will be able to substitute for the molecules of the low-molecular-mass stabilizer in the nanoparticle surface.

The presence of the stabilizer on the surface of synthesized nanoparticles was proved by IR spectroscopy. It was demonstrated for the first time that oleic acid forms an ionic bond with the surface of CdSe quantum dots,[447] and the

Scheme 4



P═O group of TOPO forms a strong coordination bond with the surface of CdS nanorods.[448]

It is evident that the process of bonding of carboxyl groups of the polymers to the nanoparticle surface in the course of substitution for low-molecular-mass stabilizer molecules should be accompanied by the rupture of cyclic associates of COOH groups (see Scheme 4). It was experimentally confirmed that the bonding of the COOH groups to the surface of CdSe quantum dots is ionic;[447] and for the nanorods initially covered with TOPO, the type of bonding with the polymer is still unknown. It is worth noting that the nanocomposite morphology is also different. Quantum dots are rather uniformly distributed over the material volume without aggregation, (Fig. 10 *a*,*b*), whereas nanorods are prone to form small domains, which tend to be homogeneously distributed over the nanocomposite volume (Fig. 10 *c*,*d*).

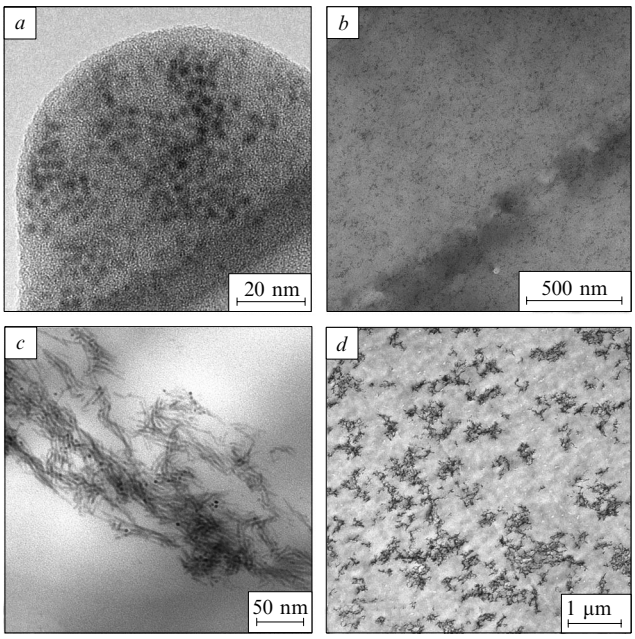


Figure 10. TEM images of the films of nanocomposites BA-6PA polymer/CdSe quantum dots (*a*, *b*) and BA-7PA polymer/CdS nanorods (*c*, *d*).[448, 449]

X-ray diffraction data have shown that nanocomposites of both types have a structure typical of BA-*n*PA polymers for which the presence of an amorphous halo is characteristic.[448, 449] The angular position of the diffraction maximum in the range $2\theta = 13-30^\circ$ corresponds to the distance between the side chains of macromolecules and does not change as nanoparticles are introduced. At the same time, quite distinguishable, even if broad, diffraction reflections appear at the shoulder of the amorphous halo at $2\theta = 25.4^\circ$ (nanocomposite with CdSe) and 27° (nanocomposite with CdS). They correspond to the (111) reflection of the cubic modification of CdSe nanocrystals and to the (002) reflection of the hexagonal modification of CdS nanocrystals.

Analysis of small-angle reflections in the X-ray diffraction patterns of nanocomposites of BA-7PA with CdSe quantum dots,[449, 450] showed that the position of the reflection corresponding to the thickness of the smectic layer of the polymer does not change with an increase in the nanoparticle content in the matrix. However, the change in the size of nanoparticles or in the length of the aliphatic pendant chain leads to the corresponding shift of this reflection. Therefore, the conclusion has been drawn that nanoparticles are introduced into the smectic layer and increase its thickness. With allowance for the fact that hydrogen-bonded groups of macromolecules are localized inside the smectic layers for which the thickness depends on the quantum dot size, a model of the nanostructure of composites of quantum dots with the LC polymer has been suggested (Fig. 11).

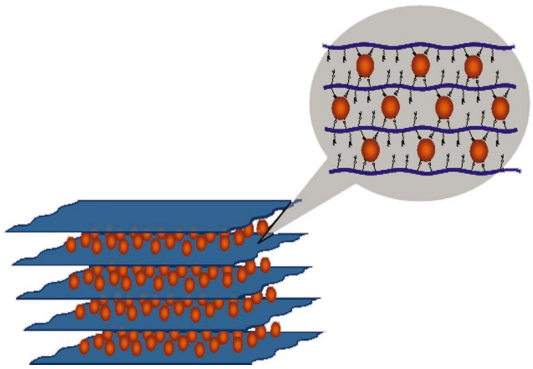


Figure 11. Model of the nanostructure of the LC polymer/CdSe quantum dots composite.[449, 450]

The notions of the nanocomposite structure are consistent with the results of studying oriented films. Uniaxial stretching of the film leads to the change of the small-angle X-ray diffraction pattern: instead of the spherical pattern for an isotropic sample, an ellipse appears with its major axis perpendicular to the stretching direction. On the basis of a set of data, the conclusion has been drawn about preferable localization of quantum dots inside the polymer layers, which are arranged parallel to the film plane upon its stretching.

As mentioned above, nanorods introduced into the LC polymer matrix form small domains distributed over the matrix volume. Uniaxial stretching of the films of such composites above the glass transition temperature with subsequent fixation of the resulting texture leads to partial coalescence of domains and to formation of long structures (Fig. 12 *a*), extended along the stretching axis. As seen from the texture X-ray diffraction pattern (Fig. 12 *b*), the polymer retains its tilted smectic structure, and the layers are also oriented along the stretching direction. The long axes of nanorods are preferably aligned in the same direction which follows from the meridional position of the (002) reflection on the small-angle electron diffraction pattern (see inset in Fig. 12 *a*).

The colour of nanocomposite films results from the luminescence properties of nanoparticles, which depend on the particle size. Figure 13 shows the luminescence spectra of the BA-6PA polymer (curve *1*), CdSe quantum dots in hexane (curve *2*) and the polymer–quantum dots composite with different filling (curves *3*–*6*). The neat polymer luminesces giving rise to two very broad lines at 400 and 510 nm of roughly the same intensity (nearly 'white' luminescence).

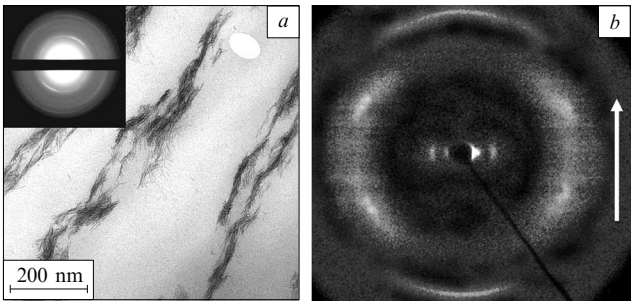


Figure 12. TEM image with the central part of the small-angle electron diffraction in the inset (*a*) and the texture X-ray diffraction pattern (*b*) of the oriented BA-7PA film with CdS nanorods.[448]

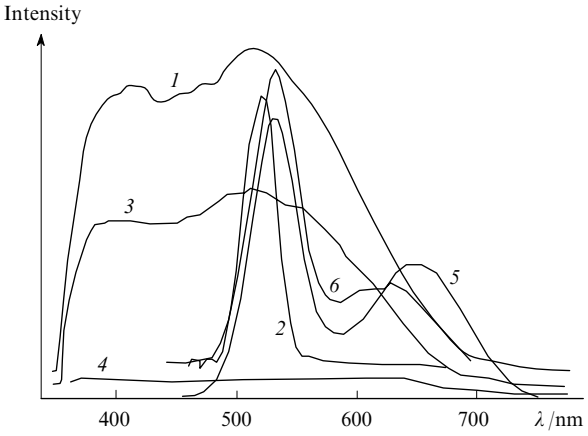


Figure 13. Luminescence spectra of the BA-6PA polymer (*1*), CdSe quantum dots in hexane (*2*) and the polymer–quantum dots nanocomposite with filling 0.5 (*3*), 5 (*4*), 10 (*5*) and 20 mass % (*6*).[450]
Radiation wavelength is 380 nm.

As the concentration of quantum dots increases from 0.05 mass % to 5 mass %, the luminescence intensity of the polymer monotonically decreases, while it seems like that the luminescence of quantum dots is lacking. However, at concentrations above 20 mass %, there appears a narrow line corresponding to the CdSe luminescence and a weaker and broader line in the red region. The first band corresponds to exciton luminescence, while the second is associated with photoluminescence of defects usually localized on the nanoparticle surface. An insignificant red shift of the major band can be attributed to the particle growth upon heat treatment, while the intrinsic luminescence of the polymer is completely quenched.

An analogous behaviour was observed for luminescence of CdS nanorods 5×50 nm in size in a solution and in the polymer matrix.[448] Figure 14 shows the absorption and photoluminescence spectra of nanorods in heptane and in the film of the LC polymer BA-10PA on exposure to light at 400 nm. Comparison of the spectra shows that the exciton peak at 468 nm for the nanorod in solution is almost not shifted in going from the solution to the polymer matrix. As in the case of quantum dots, the spectrum of the composite shows an additional weaker but significantly broader peak

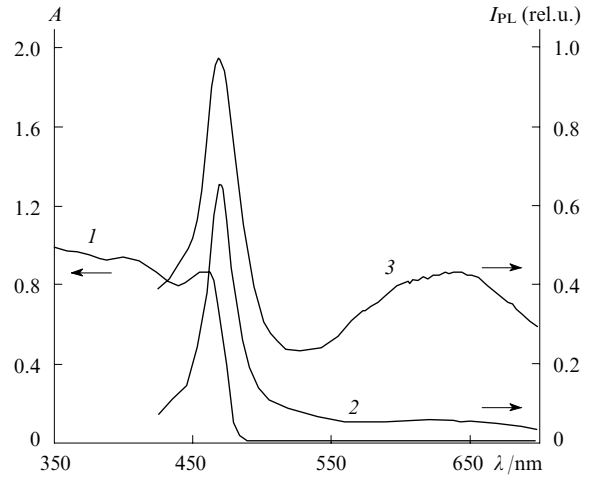


Figure 14. Absorption (*1*) and photoluminescence spectra of CdS nanorods in heptane (*2*) and in the matrix of the BA-10PA liquid-crystalline polymer (*3*) (concentration 2 mass %).[448]
Radiation wavelength is 400 nm.

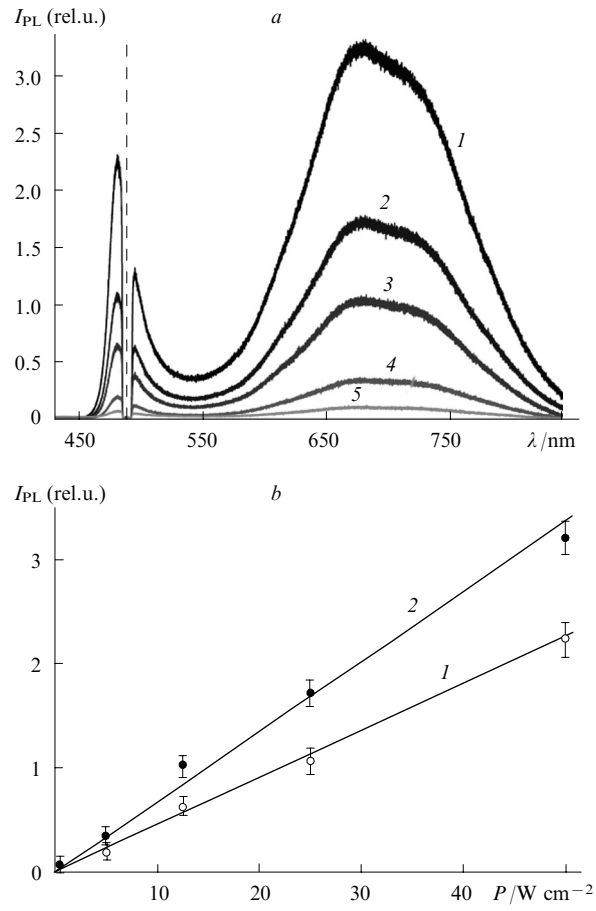


Figure 15. Photoluminescence spectra of the composite based on BA-7PA containing 33 vol.% of CdS nanorods fabricated at different densities (*P*) of excitation radiation with the wavelength 480.5 nm (*a*); *P*/W cm^{-2}: 50 (*1*), 25 (*2*), 12.5 (*3*), 5 (*4*), 0.5 (*5*).[448]
Intensities of the exciton ASPL peak (480–481 nm) (*1*) and defect photoluminescence peak (676–677 nm) (*2*) *vs.* the excitation light density (*b*).[448]

(570 – 700 mn) attributed to photoluminescence of surface defects.

When the Ag^+ laser-induced irradiation wavelength (488 nm) exceeded the luminescence wavelength, the anti-Stokes photoluminescence (ASPL) of CdS nanorods was observed for the first time. As an example, Fig. 15 *a* shows the photoluminescence spectra of the composite containing 33 vol.% of nanorods. As known, different mechanisms are available that explain ASPL, such as multiphonon excitation,[451] Auger recombination,[452] as well as different thermal mechanisms.[453] The first two processes are nonlinear in the irradiation intensity, whereas the thermal processes should be linear. Analysis of the ASPL mechanism in nanorods packed in the LC polymer matrix revealed that the intensity of both the exciton photoluminescence peak and the peak related to nanoparticle surface defects depends linearly on the radiation density (Fig. 15 *b*). This fact enabled the conclusion that ASPL of nanorods in the polymer matrix is associated with thermal processes.

Thus, polymeric LC matrices of definite structure promote self-assembly of nanoparticles in composites. Similar nanocomposites are of great interest as promising materials for optical communication systems, solid light sources based on high-brightness light-emitting diodes, biosensors and solar cells. Their optical properties are not a simple sum of the optical properties of nanoparticles and an anisotropic matrix; by contrast, the nanocomposite properties are a rather nontrivial interference of the individual properties, which is responsible for absolutely new characteristics.

VI. Conclusion

Analysis of modern literature in the fields covered by this review allows us to distinguish nanocomposites most promising from the view point of the development of new technologies. First of all, these are composites based on large-scale polyolefins or condensation polymers and organophilicized clay, in particular montmorillonite, which can be used as building materials; anticorrosion, thermoresistant and flame-proof coatings; packaging materials with decreased gas permeability; domestic cast ware. For fabrication of composites with nanodiamonds, of special interest are fluoropolymers: the composites have high wear resistance and retain the superhydrophobic properties, thermal stability and chemical inertness inherent in the neat fluoropolymer. They are widely used in various fields. Nanodiamonds are good candidates for fabrication of polymer fibers used as ion exchangers in purification of liquids and gases, as well as for subsequent graphitization and carbonization. Among conductive composites, noteworthy are highly stable electrode materials based on polyaniline and carbon nanotubes or graphite (and in the future graphene) for capacitors, power cells and other electrochemical devices. The functional characteristics of such composites can be considerably higher than those of their constituting components. Interest in materials based on LC polymers (especially chiral) and semiconductor or noble metal nanoparticles stems from their possible use in design of information processing and storage systems, in nonlinear optics, display technologies and optoelectronics.

It should be noted that the production of composites is usually a compromise between the improvement of some characteristics of the material and deterioration of the other characteristics. Properly fabricated nanomaterials avoid deterioration of properties, although they turn out to be rather expensive. Technologies for their production, or nanotechnologies, will undoubtedly find many applications, especially, in those areas where the unique properties of the material are more important than its price. However, it should not be forgotten that new technologies are usually more intricate than the old ones, so their development will require a quantum leap in the preparation of a new generation of engineers and technologists.

This review was prepared with support of a Grant of the Government of the Russian Federation for State Support of Research Conducted under the Supervision of Leading Scientists at Russian Institutions of Higher Education (Grant No. 11.G34.31.0055) and the Ministry of Education and Science of the Russian Federation in the framework of the Federal Target Programmes 'Research and Development in the Top Priority Fields of Russia's Science and Technology Complex' for 2007 – 2013 (State Contract Nos. 12.527.11.0007 and 14.518.11.7013) and 'Scientific and Scientific-Pedagogical Personnel of the Innovative Russia' for 2009 – 2013 (State Contract No. 8509).

References

1. I P Suzdalev *Nanotekhnologiya. Fiziko-khimiya Nanoklasterov, Nanostruktur i Nanomaterialov* (Nanotechnology. Physical Chemictry of Nanoclusters, Nanostructures and Nanomaterials) (Moscow: Komkniga, 2006)
2. R A Vaia, J F Maguire *Chem. Mater.* **19** 2736 (2007)
3. J E Mark *Polym. Eng. Sci.* **36** 2905 (1996)
4. A D Pomogailo *Russ. Chem. Rev.* **69** 53 (2000)
5. L M Bronstein, S N Sidorov, P M Valetsky *Russ. Chem. Rev.* **73** 501 (2004)
6. A D Pomogailo, A S Rozenberg, G I Dzhardimalieva *Russ. Chem. Rev.* **80** 257 (2011)
7. V Yu Dolmatov *Russ. Chem. Rev.* **70** 607 (2001)
8. V Yu Dolmatov *Russ. Chem. Rev.* **76** 339 (2007)
9. K Sill, S Yoo, T Emrick, in *Dekker Encyclopedia of Nanoscience and Nanotechnology* Vol. 3 (Eds J Schwarz, C I Contescu, K Putyera) (London: Taylor and Francis, 2004) p. 2999
10. P B Kocherginskaya, A V Romanova, I A Prokhorenko, D M Itkis, A V Korshun, E A Goodilin, Yu D Tretyakov *Russ. Chem. Rev.* **80** 1209 (2011)
11. M Moniruzzaman, K I Winey *Macromolecules* **39** 5194 (2006)
12. J N Coleman, U Khan, Y K Gun'ko *Adv. Mater.* **18** 689 (2006)
13. E G Rakov *Russ. Chem. Rev.* **76** 1 (2007)
14. V I Irzhak *Russ. Chem. Rev.* **80** 787 (2011)
15. E R Badamshina, M P Gafurova, Ya I Estrin *Russ. Chem. Rev.* **79** 945 (2010)
16. M A S Azizi Samir, F Alloin, A Dufresne *Biomacromolecules* **6** 612 (2005)
17. M Okamoto, in *Encyclopedia of Nanoscience and Nanotechnology* Vol. 8 (Ed. H S Nalwa) (Stevenson Ranch: American Scientific, 2004) p. 1
18. S Sinha Ray, M Bousmina *Prog. Mater. Sci.* **50** 962 (2005)
19. D R Paul, L M Robeson *Polymer* **49** 3187 (2008)
20. P Mottner, T Butz, A Lerf, G Ledezma, H Knözinger *J. Phys. Chem.* **99** 8260 (1995)
21. A K Geim, K S Novoselov *Nat. Mater.* **6** 183 (2007)
22. N Tomczak, D Jańczewski, M Han, C J Vancso *Prog. Polym. Sci.* **34** 393 (2009)
23. H Oikawa, T Onodera, A Masuhara, H Kasai, H Nakanishi *Adv. Polym. Sci.* **231** 147 (2009)
24. D H Park, M S Kim, J Joo *Chem. Soc. Rev.* **39** 2439 (2010)

25. P Alexandridis *Chem. Eng. Technol.* **34** 15 (2011)
26. A Sellinger, P M Weiss, A Nguyen, Y Lu, R A Assink, W Gong, C J Brinker *Nature (London)* **394** 256 (1998)
27. K Yamamoto, Y Sakata, Y Nohara, Y Takahashi, T Tatsumi *Science* **300** 470 (2003)
28. A A Gusev, M G Rozman *Comput. Theor. Polym. Sci.* **9** 335 (1999)
29. A A Gusev, H R Lusti *Adv. Mater.* **13** 1641 (2001)
30. A Gusev, H R Lusti, P J Hine *Adv. Eng. Mater.* **4** 927 (2002)
31. N Sheng, M C Boyce, D M Parks, G C Rutledge, J I Abes, R E Cohen *Polymer* **45** 487 (2004)
32. G A Buxton, A C Balazs *J. Chem. Phys.* **117** 7649 (2002)
33. A-C Grillet, S Brunel, Y Chevalier, S Usoni, V Ansanay-Alex, J Allemand *Polym. Int.* **53** 569 (2004)
34. H Fong, R A Vaia, J H Sanders, D Lincoln, A J Vreugdenhil, W Liu, J Bultman, C Chen *Chem. Mater.* **13** 4123 (2001)
35. H Fong, W Liu, C-S Wang, R A Vaia *Polymer* **43** 775 (2002)
36. S Pavlikováʹ, R Thomann, P Reichert, R Mülhaupt, A Marcinčin, E Borsig *J. Appl. Polym. Sci.* **89** 604 (2003)
37. B Vigloo, A Pénicaud, C Coulon, C Sauder, R Pailler, C Journet, P Bernier, P Poulin *Science* **290** 1331 (2003)
38. S Kumar, T D Dang, F E Arnold, A R Bhattacharyya, B G Min, X Zhang, R A Vaia, C Park, W W Adams, R H Hauge, R E Smalley, S Ramesh, P A Willis *Macromolecules* **35** 9039 (2002)
39. T E Dirama, L A Goettler *Mater. Manufact. Process.* **21** 199 (2006)
40. J W Cho, D R Paul *Polymer* **42** 1083 (2001)
41. R Krishnamoorti, K Yurekli *Curr. Opin. Colloid Interface Sci.* **6** 464 (2001)
42. G Schmidt, A I Nakatani, P D Butler, A Karim, C C Han *Macromolecules* **33** 7219 (2000)
43. H Koerner, E Hampton, D Dean, Z Turgut, L Drummy, P Mirau, R Vaia *Chem. Mater.* **17** 1990 (2005)
44. M J Casavant, D A Walters, J J Schmidt, R E Smalley *J. Appl. Phys.* **93** 2153 (2003)
45. H Koerner, J D Jacobs, D W Tomlin, J Busbee, R A Vaia *Adv. Mater.* **16** 297 (2004)
46. L E Nilsen *Mechanical Properties of Polymers and Composites* (New York: Marcel Dekker, 1974)
47. Yu S Lipatov *Fizicheskaya Khimiya Napolnennykh Polimerov* (Physical Chemistry of Filled Polymers) (Moscow: Khimiya, 1977)
48. J A Manson, L H Sperling *Polymer Blends and Composites* (New York: Plenum Press, 1976)
49. M Sumita, Y Tsukumo, K Miyasaka, K Ishikawa *J. Mater. Sci.* **18** 1758 (1983)
50. M Hussain, A Nakahira, S Nishijima, K Niihara *Mater. Lett.* **27** 21 (1996)
51. M Sumita, H Tsukihi, K Miyasaka, K Ishikawa *J. Appl. Polym. Sci.* **29** 1523 (1984)
52. K-t Lau, C Gu, D Hui *Composites, Part B: Eng.* **37** 425 (2006)
53. H-S Lee, P D Fasulo, W R Rodgers, D R Paul *Polymer* **46** 11673 (2005)
54. J Markarian *Plast., Addit. Compound.* **7** (6) 18 (2005)
55. Z S Petrović, I Javni, A Waddon, G Bánhegyi *J. Appl. Polym. Sci.* **76** 133 (2000)
56. Z S Petrović, W Zhang *Mater. Sci. Forum* **352** 171 (2000)
57. K Friedrich, U A Karsch *Fibre Sci. Technol.* **18** 37 (1983)
58. F C Wong, A Ait-Kadi *J. Appl. Polym. Sci.* **55** 263 (1995)
59. V A Topolkaraev, Yu M Tovmasyan, I L Dubnikova, A I Petrosyan, I N Meshkova, A A Berlin, N S Enikolopyan *Dokl. Akad. Nauk SSSR* **290** 1418 (1986) [a]
60. A N Gent *Rubber Chem. Technol.* **56** 1011 (1983)
61. S E Evlampieva, in *Deformirovanie i Razrushenie Kompozitov* (Deformation and Destruction of Composite Materials) (Ed. Yu V Sokolkin) (Sverdlovsk: Ural Scientific Centre, Academy of Sciences of the USSR, 1985) p. 8
62. S Ahmed, F R Jones *J. Mater. Sci.* **25** 4933 (1990)
63. D M Bigg *Polym. Compos.* **8** 115 (1987)
64. J E Ashton, J C Halpin, P H Petit *Primer on Composite Materials: Analysis* (Stamford: Technomic, 1969)
65. M van Es, F Xiqiao, J van Turnhout, E van der Giessen, in *Specialty Polymer Additives: Principles and Applications* (Eds S Al-Malaika, A W Golovoy, C A Wilkie) (Malden: Blackwell, 2001) p. 512
66. D Hull, T W Clyne *An Introduction to Composite Materials* (2nd Ed.) (New York: Cambridge University Press, 1996)
67. M Alexandre, P Dubois *Mater. Sci. Eng. R* **28** 1 (2000)
68. S Sinha Ray, M Okamoto *Prog. Polym. Sci.* **28** 1539 (2003)
69. R E Grim *Clay Mineralogy* (New York: McGraw-Hill, 1953)
70. V P Kovrigo, I S Kaurichev, L M Burlakova *Pochvovedenie s Osnovami Geologii* (Soil Sience and Fundamentals of Geology) (Moscow: Kolos, 2000)
71. L A Utracki *Clay-Containing Polymeric Nanocomposites* Vol. 1 (Shawbury: Rapra Technology, 2004)
72. S Pavlidou, C D Papaspyrides *Prog. Polym. Sci.* **33** 1119 (2008)
73. F Gao *Mater. Today* **7** (11) 50 (2004)
74. J Zhang, E Manias, C A Wilkie *J. Nanosci. Nanotechnol.* **8** 1597 (2008)
75. M Šupováʹ, G S Martynkováʹ, K Barabaszováʹ *Sci. Adv. Mater.* **3** 1 (2011)
76. P M Ajayan, L S Schadler, P V Braun *Nanocomposite Science and Technology* (Weinheim: Wiley, 2003)
77. Y C Ke, P Stroeve *Polymer-Layered Silicate and Silica Nanocomposites* (Amsterdam, Oxford, New York: Elsevier, 2005)
78. A V Ivanyuk, O A Adrov, V A Gerasin, M A Guseva, H R Fischer, E M Antipov *Vysokomol. Soedin., Ser. A* **46** 1945 (2004) [b]
79. A V Ivanyuk, V A Gerasin, A V Rebrov, R G Pavelko, E M Antipov *Inzh.-Fiz. Zh.* **78** (5) 87 (2005) [c]
80. E M Antipov, M A Guseva, V A Gerasin, Yu M Korolev, A V Rebrov, H R Fischer, I V Razumovskaya *Vysokomol. Soedinen., Ser. A* **45** 1874 (2003) [b]
81. E M Antipov, A A Barannikov, V A Gerasin, B F Shklyaruk, L A Tsamalashvili, H R Fischer *Vysokomol. Soedin., Ser. A* **45** 1885 (2003) [b]
82. *Dekker Encyclopedia of Nanoscience and Nanotechnology* (Eds C I Contescu, K Putyera) (New York: Marcel Dekker, 2004)
83. *The X-ray Identification and Crystal Structures of Clay Minerals* (Ed. G Brown) (Mineralogical Society, Clay Minerals Group, 1951)
84. B K G Theng *Formation and Properties of Clay-Polymer Complexes* (Amsterdam, Oxford, New York: Elsevier, 1979)
85. *Rentgenografiya Osnovnykh Tipov Porodoobrazuyushchikh Mineralov* (X-Ray Imaging of Basic Types of Rock Forming Minerals) (Ed. V A Frank-Kamenetsky) (Leningrad: Nedra, 1983)
86. E G Kukovskii *Prevrashcheniya Sloistykh Silikatov* (Transformations of Layered Silicates) (Kiev: Naukova Dumka, 1973)
87. A Meunier *Clays* (Berlin, Heidelberg, New York: Springer, 2005)
88. A R Mermut, G Lagaly *Clays Clay Miner.* **49** 393 (2001)
89. R E Grim, G Kulbicki *Am. Mineral.* **46** 1329 (1961)
90. *Gruntovedenie* (Ground Science) (Ed. V T Trofimov) (Moscow: Moscow State University, 2005)
91. Yu G Frolov *Kurs Kolloidnoi Khimii* (The Course of Colloidal Chemistry) (Moscow: Khimiya, 1982)
92. C E Weaver, L D Pollard *The Chemistry of Clay Minerals* (Oxford: Elsevier, 1975)
93. J R Sohn, S I Lee *Langmuir* **16** 5024 (2000)
94. J R Sohn, J T Kim *Langmuir* **16** 5430 (2000)
95. X Ding, S M Henrichs *Mar. Chem.* **77** 225 (2002)

96. D M K Mak-Yuan, in *The X-ray Identification and Crystal Structures of Clay Minerals* (Ed. G Brown) (Mineralogical Society, Clay Minerals Group, 1951) p. 177
97. Y-H Yu, C-Y Lin, J-M Yeh, W-H Lin *Polymer* **44** 3553 (2003)
98. A Farkas, I Dékány *Colloid Polym. Sci.* **279** 459 (2001)
99. B Liao, M Song, H Liang, Y Pang *Polymer* **42** 10007 (2001)
100. S-J Park, D-I Seo, J-R Lee *J. Colloid Interface Sci.* **251** 160 (2002)
101. W W Emerson, M Raupach *Aust. J. Soil Res.* **2** 46 (1964)
102. O Griot, J A Kitchener *Trans. Faraday Soc.* **61** 1032 (1965)
103. S Yamanaka, F Kanamaru, M Koizumi *J. Phys. Chem.* **79** 1285 (1975)
104. A S Michaels, O Morelos *Ind. Eng. Chem.* **47** 1801 (1955)
105. R A Ruehrwein, D W Ward *Soil Sci.* **73** 485 (1952)
106. I A Uskov, Yu G Tarasenko, T A Kusnitsyna *Vysokomol. Soedin.* **3** 37 (1961) [b]
107. A Maftuleac, I Dranca, T Lupascu *J. Therm. Anal. Calorim.* **69** 589 (2002)
108. W Shen, H He, J Zhu, P Yuan, R L Frost *J. Colloid Interface Sci.* **313** 268 (2007)
109. H He, J Duchet, J Galy, J-F Gerard *J. Colloid Interface Sci.* **288** 171 (2005)
110. N V Gudovich, F D Ovcharenko *Kolloid. Zh.* **25** 407 (1963) [d]
111. S Šnircová, E Jóna, L Lajdová, V Jorik, M Drábik, M Pajtášová, D Ondrušová, S C Mojumdar *J. Therm. Anal. Calorim.* **96** 63 (2009)
112. J-H Yang,Y-S Han, J-H Choy, H Tateyama *J. Mater. Chem.* **11** 1305 (2001)
113. G Lagaly *Solid State Ionics* **22** 43 (1986)
114. B K G Theng *The Chemistry of Clay-Organic Reactions* (London: Adam Hilger, 1974)
115. S Akyüz, T Akyüz, A E J Yakar *J. Mol. Struct.* **565 – 566** 487 (2001)
116. S Akyüz, T Akyüz, J E D Davies *J. Mol. Struct.* **482 – 483** 49 (1999)
117. S Sen, N Nugay, T Nugay *e-Polymers* 049 (2003)
118. B H Kim, J H Jung, J W Kim, H J Choi, J Joo *Synth. Met.* **117** 115 (2001)
119. A I Serdyuk, R V Kucher *Mitsellyarnye Perekhody v Rastvorakh Poverkhnostno-aktivnykh Veshchestv* (Micellar Transitions in Surfactant Solutions) (Kiev: Naukova Dumka, 1987)
120. Yu I Tarasevich, F D Ovcharenko *Adsorbtsiya na Glinistykh Mineralakh* (Adsorption on Clay Minerals) (Kiev: Naukova Dumka, 1975)
121. P Reichert, J Kressler, R Thomann, R Müllhaupt, G Stöppelmann *Acta Polym.* **49** 116 (1998)
122. T D Fornes, P J Yoona, D L Hunter, H Keskkula, D R Paul *Polymer* **43** 5915 (2002)
123. L Le Pluart, J Duchet, H Sautereau *Polymer* **46** 12267 (2005)
124. H He, R L Frost, T Bostrom, P Yuan, L Duong, D Yang, Y Xi, J T Kloprogge *Appl. Clay Sci.* **31** 262 (2006)
125. R A Vaia, R K Teukolsky, E P Giannelis *Chem. Mater.* **6** 1017 (1994)
126. W Xiao, M Zhan, Z Li *Mater. Des.* **24** 455 (2003)
127. M Fermeglia, M Ferrone, S Pricl *Fluid Phase Equilibr.* **212** 315 (2003)
128. V Kuppa, T M D Foley, E Manias *Eur. Phys. J. E* **12** 159 (2003)
129. V A Gerasin, F N Bakhov, N D Merekalova, Yu M Korolev, H R Fischer, E M Antipov *Vysokomol. Soedin., Ser. A* **47** 1635 (2005) [b]
130. V A Gerasin, T A Zubova, F N Bakhov, A A Barannikov, N D Merekalova, Yu M Korolev, E M Antipov *Ros. Nanotekhnol.* **2** (1 – 2) 90 (2007) [e]
131. K A Prokhorov, E A Saguitova, G Yu Nikolaeva, D N Kozlov, P P Pashinin, E M Antipov, V A Gerasin, F N Bakhov, M A Guseva *Laser Phys. Lett.* **2** 285 (2005)
132. Z P Luo, J H Koo *Polymer* **49** 1841 (2008)
133. R Wagener, T J G Reisinger *Polymer* **44** 7513 (2003)
134. R Krishnamoorti, J Ren, A S Silva *J. Chem. Phys.* **114** 4968 (2001)
135. R Krishnamoorti, E P Giannelis *Macromolecules* **30** 4097 (1997)
136. R A Vaia, E P Giannelis *Macromolecules* **30** 7990 (1997)
137. R A Vaia, E P Giannelis *Macromolecules* **30** 8000 (1997)
138. V V Ginzburg, A C Balazs *Adv. Mater.* **12** 1805 (2000)
139. V V Ginzburg, J D Weinhold, P K Jog, R Srivastava *Macromolecules* **42** 9089 (2009)
140. V V Ginzburg, C Singh, A C Balazs *Macromolecules* **33** 1089 (2000)
141. Y Lyatskaya, A C Balazs *Macromolecules* **31** 6676 (1998)
142. A C Balazs, C Singh, E Zhulina *Macromolecules* **31** 8370 (1998)
143. A C Balazs, C Singh, E Zhulina, Y Lyatskaya *Acc. Chem. Res.* **32** 651 (1999)
144. Y V Kudryavtsev, E N Govorun, A D Litmanovich, H R Fischer *Macromol. Theor. Simul.* **13** 392 (2004)
145. H Fischer *Mater. Sci. Eng., C* **23** 763 (2003)
146. K Chrissopoulou, I Altintzi, S H Anastasiadis, E P Giannelis, M Pitsikalis, N Hadjichristidis, N Theophilou *Polymer* **46** 12440 (2005)
147. T S Gates, G M Odegard, S J V Frankland, T C Clancy *Compos. Sci. Technol.* **65** 2416 (2005)
148. G M Odegard, T C Clancy, T S Gates *Polymer* **46** 553 (2005)
149. J Jancar, J F Douglas, F W Starr, S K Kumar, P Cassagnau, A J Lesser, S S Sternstein, M J Buehler *Polymer* **51** 3321 (2010)
150. G Scocchi, P Posocco, A Danani, S Pricl, M Fermeglia *Fluid Phase Equilibr.* **261** 366 (2007)
151. M Fermeglia, S Pricl *Comput. Chem. Eng.* **33** 1701 (2009)
152. Q H Zeng, A B Yu, G Q Lu *Prog. Polym. Sci.* **33** 191 (2008)
153. D J Greenland *J. Colloid Sci.* **18** 647 (1963)
154. N Ogata, S Kawakage, T Ogihara *J. Appl. Polym. Sci.* **66** 573 (1997)
155. N Ogata, S Kawakage, T Ogihara *Polymer* **38** 5115 (1997)
156. R L Parfitt, D J Greenland *Clay Miner.* **8** 305 (1970)
157. X Zhao, K Urano, S Ogasawara *Colloid Polym. Sci.* **267** 899 (1989)
158. J Billingham, C Breen, J Yarwood *Vib. Spectrosc.* **14** 19 (1997)
159. E Ruiz-Hitzky, B Casal, P Aranda, J C Galvvn *Rev. Inorg. Chem.* **21** 125 (2001)
160. R Levy, C Francis *J. Colloid Interface Sci.* **50** 442 (1975)
161. J Wu, M M Lerner *Chem. Mater.* **5** 835 (1993)
162. D C Lee, L W Jang *J. Appl. Polym. Sci.* **61** 1117 (1996)
163. M W Noh, D C Lee *Polym. Bull.* **42** 619 (1999)
164. T Lan, P D Kaviratna, T J Pinnavaia *Chem. Mater.* **6** 573 (1994)
165. K Yano, A Usuki, A Okada, T Kurauchi, O Kamigaito *J. Polym. Sci., Part A: Polym. Chem.* **31** 2493 (1993)
166. Y Fukushima, A Okada, M Kawasumi, T Kurauchi, O Kamigaito *Clay Miner.* **23** 27 (1988)
167. A Usuki, Y Kojima, M Kawasumi, A Okada, Y Fukushima, T Kurauchi, O Kamigaito *J. Mater. Res.* **8** 1179 (1993)
168. C Zilg, R Mülhaupt, J Finter *Macromol. Chem. Phys.* **200** 661 (1999)
169. H G Jeon, H-T Jung, S W Lee, S D Hudson *Polym. Bull.* **41** 107 (1998)
170. N Ogata, G Jimenez, H Kawai, T Ogihara *J. Polym. Sci., Part B: Polym. Phys.* **35** 389 (1997)
171. G Jimenez, N Ogata, H Kawai, T Ogihara *J. Appl. Polym. Sci.* **64** 2211 (1997)
172. R A Vaia Ph.D. Thesis, Cornell University, Ithaca, NY, 1995
173. D Wolf, U Wagenknecht, B Kretzschmar, in *Interface Controlled Materials (EUROMAT* Vol. 9) (Eds M Rühle H Gleiter) (Weinheim: Wiley-VCH, 2005) p. 189

174. E Manias, A Touny, L Wu, K Strawhecker, B Lu, T C Chung *Chem. Mater.* **13** 3516 (2001)
175. N Hasegawa, M Kawasumi, M Kato, A Usuki, A Okada *J. Appl. Polym. Sci.* **67** 87 (1998)
176. S Mehta, F M Mirabella, K Rufener, A Bafna *J. Appl. Polym. Sci.* **92** 928 (2004)
177. D Kämpfer, R Thomann, R Mülhaupt *Polymer* **43** 2909 (2002)
178. A B Morgan, J D Harris *Polymer* **44** 2313 (2003)
179. N Hasegawa, A Usuki *J. Appl. Polym. Sci.* **93** 464 (2004)
180. W Xu, G Liang, H Zhai, S Tang, G Hang, W-P Pan *Eur. Polym. J.* **39** 1467 (2003)
181. C Danumah, M Bousmina, S Kaliaguine *Macromolecules* **36** 8208 (2003)
182. Z M Wang, H Nakajima, E Manias, T C Chung *Macromolecules* **36** 8919 (2003)
183. J Heinemann, P Reichert, R Thomann, R Mülhaupt *Macromol. Rapid Commun.* **20** 423 (1999)
184. M Alexandre, P Dubois, T Sun, J M Garces, R Jérôme *Polymer* **43** 2123 (2002)
185. S-Y A Shing, L C Simon, J B P Soares, G Scholz *Polymer* **44** 5317 (2003)
186. F Yang, X Zhang, H Zhao, B Chen, B Huang, Z Feng *J. Appl. Polym. Sci.* **89** 3680 (2003)
187. C Liu, T Tang, D Wang, B Huang *J. Polym. Sci., Part A: Polym. Chem.* **41** 2187 (2003)
188. Patent US 5910523 (1999)
189. Y Kojima, A Usuki, M Kawasumi, A Okada, T Kurauchi, O Kamigaito *J. Polym. Sci., Part A: Polym. Chem.* **31** 1755 (1993)
190. Y Kojima, A Usuki, M Kawasumi, A Okada, T Kurauchi, O Kamigaito *J. Polym. Sci., Part A: Polym. Chem.* **31** 983 (1993)
191. Y Kojima, A Usuki, M Kawasumi, A Okada, Y Fukushima, T Kurauchi, O Kamigaito *J. Mater. Res.* **8** 1185 (1993)
192. L Liu, Z Qi, X Zhu *J. Appl. Polym. Sci.* **71** 1133 (1999)
193. G Lagaly, in *Development in Ionic Polymers* (Eds A D Wilson, H J Prosser) (London: Elsevier, 1986) p. 77
194. G P Cherepanov *Mekhanika Khrupkogo Razrusheniya* (Mechanics of Brittle Destruction) (Moscow: Nauka, 1974)
195. Y Yang, Z-k Zhu, J Yin, X-y Wang, Z-e Qi *Polymer* **40** 4407 (1999)
196. S Bazhenov *J. Mater. Sci.* **32** 797 (1997)
197. O K Garishin, A L Svistkov, V A Gerasin, M A Guseva *Vysokomol. Soedin., Ser. A* **51** 610 (2009) [b]
198. A Bafna, G Beaucage, F Mirabella, S Mehta *Polymer* **44** 1103 (2003)
199. G Galgali, S Agarwal, A Lele *Polymer* **45** 6059 (2004)
200. M E Mackay, T T Dao, A Tuteja, D L Ho, B Van Horn, H-C Kim, C J Hawker *Nat. Mater.* **2** 762 (2003)
201. R Tuinier, J K G Dhont, T-H Fan *Europhys. Lett.* **75** 929 (2006)
202. T-H Fan, J K G Dhont, R Tuinier *Phys. Rev. E* **75** 011803 (2007)
203. M Wang, R J Hill *Soft Matter* **5** 3940 (2009)
204. A Tuteja, M E Mackay, C J Hawker, B Van Horn *Macromolecules* **38** 8000 (2005)
205. T-H Fan, R Tuinier *Soft Matter* **6** 647 (2010)
206. B Hoffmann, J Kressler, G Stöppelmann, C Friedrich, G -M Kim *Colloid Polym. Sci.* **278** 629 (2000)
207. J Li, C Zhou, G Wang, D Zhao *J. Appl. Polym. Sci.* **89** 3609 (2003)
208. P J Yoon, D L Hunter, D R Paul *Polymer* **44** 5341 (2003)
209. A Riva, M Zanetti, M Braglia, G Camino, L Falqui *Polym. Degrad. Stab.* **77** 299 (2002)
210. RF P. 2424797 (2011)
211. K Iakoubovskii, M V Baidakova, B H Wouters, A Stesmans, G J Adriaenssens, A Ya Vul', P J Grobet *Diamond Relat. Mater.* **9** 861 (2000)
212. V V Danilenko *Fiz. Tv. Tela* **46** 581 (2004) [f]
213. G Post, V Yu Dolmatov, V A Marchukov, V G Sushchev, M V Veretennikova, A E Sal'ko *Zh. Prikl. Khim.* **75** 773 (2002) [g]
214. V Yu Dolmatov, M V Veretennikova, V A Marchukov, V G Sushchev *Fiz. Tv. Tela* **46** 596 (2004) [f]
215. *Synthesis, Properties and Applications of Ultrananocrystalline Diamond (NATO Sci. Ser.* Vol. 192) (Eds D M Gruen, O A Shenderova, A Ya Vul') (New York: Springer, 2005)
216. I I Kulakova *Fiz. Tv. Tela* **46** 621 (2004) [f]
217. A P Rudenko, I I Kulakova, V L Skvortsova *Russ. Chem. Rev.* **62** 87 (1993)
218. O A Shenderova, V V Zhirnov, D W Brenner *Crit. Rev. Solid State Mater. Sci.* **27** 227 (2002)
219. A Yu Neverovskaya, A P Voznyakovskii, V Yu Dolmatov *Fiz. Tv. Tela* **46** 646 (2004) [f]
220. Y W Zhu, X Q Shen, B C Wang, X Y Xu, Z J Feng *Fiz. Tv. Tela* **46** 665 (2004) [f]
221. K Xu, Q Xue *Fiz. Tv. Tela* **46** 633 (2004) [f]
222. S I Chukhaeva *Fiz. Tv. Tela* **46** 610 (2004) [f]
223. V S Bondar', A P Puzyr' *Fiz. Tv. Tela* **46** 698 (2004) [f]
224. A P Puzyr', G E Selyutin, V B Vorob'ev, E N Fedorova, K V Purtov, V A Voroshilov, V S Bondar' *Nanotekhnika* (4) 96 (2006)
225. I I Kulakova *Ros. Khim. Zh.* **48** (5) 97 (2004) [h]
226. L V Agibalova, A P Voznyakovskii, V Yu Dolmatov, V V Klyubin *Sverkhtv. Mater.* **4** 87 (1998) [i]
227. P A Vityaz' *Fiz. Tv. Tela* **46** 591 (2004) [f]
228. N V Novikov, G P Bogatyreva, M N Voloshin *Fiz. Tv. Tela* **46** 585 (2004) [f]
229. G P Bogatyreva, M A Marinich, E V Ishchenko, V L Gvyazdovskaya, G A Bazalii, N A Oleinik *Fiz. Tv. Tela* **46** 718 (2004) [f]
230. V Yu Dolmatov, T Fujimura, G K Burkat, E A Orlova, M V Veretennikova *Powder Metall. Met. Ceram.* **42** 587 (2003)
231. G N Yushin, S Osswald, V I Padalko, G P Bogatyreva, Y Gogotsi *Diamond Relat. Mater.* **14** 1721 (2005)
232. M A Ray, O Shenderova, W Hook, A Martin, V Grishko, T Tyler, G B Cunningham, G McGuire *Diamond Relat. Mater.* **15** 1809 (2006)
233. A P Puzyr', I O Pozdnyakova, V S Bondar' *Fiz. Tv. Tela* **46** 740 (2004) [f]
234. H Huang, E Pierstorff, E Osawa, D Ho *Nano Lett.* **7** 3305 (2007)
235. Patent RF 2203068 (2003)
236. V S Bondar', I O Pozdnyakova, A P Puzyr' *Fiz. Tv. Tela* **46** 737 (2004) [f]
237. A P Puzyr, D A Neshumayev, S V Tarskikh, G V Makarskaya, V Yu Dolmatov, V S Bondar *Diamond Relat. Mater.* **13** 2020 (2004)
238. A P Puzyr, V Yu Dolmatov, I V Shugalei, D A Neshumayev, S V Tarskikh, G V Makarskaya, V S Bondar, N P Dubyago, in *Innovative Superhard Materials and Sustainable Coatings for Advanced Manufacturing (NATO Sci. Ser. Ser II* Vol. 200) (Eds J Lee, N Novikov) (Springer, 2005) p. 155
239. A P Voznyakovskii, L F Shelokhneva, V Yu Dolmatov, V S Bodrova *Kauch. Rezina* (6) 27 (1996)
240. I I Konstantinov, V V Karbushev, A V Semakov, V G Kulichikhin *Zh. Prikl. Khim.* **82** 489 (2009) [g]
241. V V Karbushev, A V Semakov, V G Kulichikhin *Vysokomol. Soedin., Ser. A* **53** 1513 (2011) [b]
242. V G Kulichikhin, A V Semakov, V V Karbushev, N A Plate, S J Picken *Vysokomol. Soedin.* **51** 2044 (2009) [b]
243. V Kulichikhin, A Semakov, V Karbushev, V Makarova, E Mendes, H Fisher, S Picken, in *Advances in Nanocomposites — Synthesis Characterization and Industrial Applications* (Ed. B Reddy) (InTech, 2011) p. 227

244. A P Korobko, S V Krasheninnikov, I V Levakova, L A Ozerina, S N Chvalun *Vysokomol. Soedin., Ser. A* **43** 1984 (2001) [b]
245. U Maitra, K E Prasad, U Ramamurty, C N R Rao *Solid State Commun.* **149** 1693 (2009)
246. T S Kurkin, A N Ozerin, A S Kechek'yan, L A Ozerina, E S Obolonkova, M A Beshenko, V Yu Dolmatov *Vysokomol. Soedin., Ser. A* **50** 54 (2008) [b]
247. V Yu Dolmatov *J. Superhard Mater.* **29** 1 (2007)
248. A M Firsov, E A Petrov, V V Ruzhikov, R O Bragin, in *The 3rd International Symposium on Detonation Nanodiamonds: Production, Properties, Applications, St Petersburg, 2003* p. 112
249. O Shenderova, T Tyler, G Cunningham, M Ray, J Walsh, M Casulli, S Hens, G McGuire, V Kuznetsov, S Lipa *Diamond Relat. Mater.* **16** 1213 (2007)
250. T Tyler, O Shenderova, G Cunningham, J Walsh, J Drobnik, G McGuire *Diamond Relat. Mater.* **15** 2078 (2006)
251. Q Zhang, K Naito, Y Tanaka, Y Kagawa *Macromol. Rapid Commun.* **28** 2069 (2007)
252. Q Zhang, K Naito, Y Tanaka, Y Kagawa *Macromolecules* **41** 536 (2008)
253. A P Korobko, Yu M Milekhin, S V Krasheninnikov, N I Shishov, I V Levakova, S N Chvalun, L A Ozerina, T A Bestuzheva, S N Drozd, E A Butenko *Vysokomol. Soedinen., Ser. A* **46** 1558 (2004) [b]
254. A Stravato, R Knight, V Mochalin, S C Picardi *J. Therm. Spray Technol.* **17** 812 (2008)
255. L Bilogurova, M Shevtsova *Materialwiss. Werkstofftech.* **40** 331 (2009)
256. K D Behler, A Stravato, V Mochalin, G Korneva, G Yushin, Y Gogotsi *ACS Nano* **3** 363 (2009)
257. A P Korobko, N P Bessonova, S V Krasheninnikov, E V Konyukhova, S N Drozd, S N Chvalun *Diamond Relat. Mater.* **16** 2141 (2007)
258. A P Voznyakovskii *Fiz. Tv. Tela* **46** 629 (2004) [f]
259. N V Sirotinkin, A P Voznyakovskii, A N Ershova *Fiz. Tv. Tela* **46** 725 (2004) [f]
260. V Yu Dolmatov *J. Superhard Mater.* **29** 65 (2007)
261. A P Voznyakovskii, A S Ramsh, V Yu Dolmatov, N F Kovalev, V S Bodrova, L S Shelokhneva *Kauch. Rezina* (1) 6 (1998)
262. L A Akopyan, M N Zlotnikov, B V Rumyantsev, N L Abramova, M V Zobina, T L Mordvintseva *Fiz. Tv. Tela* **46** 722 (2004) [f]
263. J-Y Lee, D-S Lim *Surf. Coat. Technol.* **188 – 189** 534 (2004)
264. A P Voznyakovskii, B M Ginzburg, D Rashidov, D G Tochil'nikov, Sh Tuichiev *Vysokomol. Soedin., Ser. A* **52** 1790 (2010) [b]
265. S Iijima *Nature (London)* **354** 56 (1991)
266. M A Hamon, J Chen, H Hu, Y Chen, M E Itkis, A M Rao, P C Eklund, R C Haddon *Adv. Mater.* **11** 834 (1999)
267. J E Riggs, Z Guo, D L Carroll, Y-P Sun *J. Am. Chem. Soc.* **122** 5879 (2000)
268. K Lota, V Khomenko, E Frackowiak *J. Phys. Chem. Solids* **65** 295 (2004)
269. I Sapurina, J Stejskal *Polym. Int.* **57** 1295 (2008)
270. A G MacDiarmid, W E Jones Jr , I D Norris, J Gao, A T Jonson Jr, N J Pinto, J Hone, B Han, F K Ko, H Okuzaki, M Llaguno *Synth. Met.* **119** 27 (2001)
271. I Yu Sapurina, J Stejskal *Russ. Chem. Rev.* **79** 1123 (2010)
272. L Jin, C Bower, O Zhou *Appl. Phys. Lett.* **73** 1197 (1998)
273. Z Jin, K P Pramoda, G Xu, S H Goh *Chem. Phys. Lett.* **337** 43 (2001)
274. H Zengin, W Zhow, J Jin, R Czerw, D W Smith Jr, L Echegoyen, D L Carroll, S H Foulger, J Ballato *Adv. Mater.* **14** 1480 (2002)
275. G Cheng, J Zhao, Y Tu, P He, Y Fang *Anal. Chim. Acta* **533** 11 (2005)
276. F Qu, M Yang, J Jiang, G Shen, R Yu *Anal. Biochem.* **344** 108 (2005)
277. Z Jia, Z Wang, C Xu, J Liang, B Wei, D Wu, S Zhu *Mater. Sci. Eng., A* **271** 395 (1999)
278. H T Ham,Y S Choi, N Jeong, I J Chung *Polymer* **46** 6308 (2005)
279. X Zhang, J Zhang, Z Liu *Appl. Phys. A: Mater. Sci. Process.* **80** 1813 (2005)
280. R Sainz, A M Benito, M T Martínez, J F Galindo, J Sotres, A M Baró, B Corraze, O Chauvet, W K Maser *Adv. Mater.* **17** 278 (2005)
281. M Cochet, W K Maser, A M Benito, M A Callejas, M T Martínez, J-M Benoit, J Schreiber, O Chauvet *Chem. Commun.* 1450 (2001)
282. M Deng, B Yang, Y Hu *J. Mater. Sci.* **40** 5021 (2005)
283. Y Yu, B Che, Z Si, L Li, W Chen, G Xue *Synth. Met.* **150** 271 (2005)
284. B Philip, J Xie, J K Abraham, V K Varadan *Polym. Bull.* **53** 127 (2005)
285. C Park, Z Ounaies, K A Watson, R E Crooks, J Smith Jr, S E Lowther, J W Connell, E J Siochi, J S Harrison, T L St Clair *Chem. Phys. Lett.* **364** 303 (2002)
286. A V Okotrub, I P Asanov, P S Galkin, L G Bulusheva, G N Chekhova, A G Kurenya, Yu V Shubin *Vysokomol. Soedinen., Ser. B* **52** 351 (2010) [b]
287. E N Konyushenko, J Stejskal, M Trchová, J Hradil, J Kovářová, J ProkesP, M Cieslar, J-Y Hwang, K-H Chen, I Sapurina *Polymer* **47** 5715 (2006)
288. T Jeevananda, Siddaramaiah, T S Lee, J H Lee, O M Samir, R Somashekar *J. Appl. Polym. Sci.* **109** 200 (2008)
289. E Zelikman, M Narkis, A Siegmann, L Valentini, J M Kenny *Polym. Eng. Sci.* **48** 1872 (2008)
290. P J Kinlen, J Liu, Y Ding, C R Graham, E E Remsen *Macromolecules* **31** 1735 (1998)
291. J Kim, S Kwon, D W Ihm *Curr. Appl. Phys.* **7** 205 (2007)
292. M Ginik-Markovic, J G Matisons, R Cervini, G P Simon, P M Fredericks *Chem. Mater.* **18** 6258 (2006)
293. R Y Suckeveriene, E Zelikman, G Mechrez, A Tzur, I Frisman, Y Cohen, M Narkis *J. Appl. Polym. Sci* **120** 676 (2011)
294. E Zelikman, R Y Suckeveriene, G Mechrez, M Narkis *Polym. Adv. Technol.* **21** 150 (2010)
295. S Hong, M Kim, C K Hong, D Jung, S E Shim *Synth. Met.* **158** 900 (2008)
296. B G Soares, M E Leyva, G M O Barra, D Khastgir *Eur. Polym. J.* **42** 676 (2006)
297. Y Huang, S Jiang, L Wu, Y Hua *Polym. Test.* **23** 9 (2004)
298. H Zhang, H X Li, H M Cheng *J. Phys. Chem. B* **110** 9095 (2006)
299. M Yang, V Koutsos, M Zaiser *J. Phys. Chem. B* **109** 10009 (2005)
300. A V Orlov, S G Kiseleva, O Yu Yurchenko, G P Karpacheva *Vysokomol. Soedin., Ser. A* **42** 2089 (2000) [b]
301. A V Orlov, S G Kiseleva, G P Karpacheva, V V Teplyakov, D A Syrtsova, L E Starannikova, T E Lebedeva *J. Appl. Polym. Sci.* **89** 1379 (2003)
302. Y Wei, Y Sun, X Tang *J. Phys. Chem.* **93** 4878 (1989)
303. V V Abalyaeva, V R Bogatyrenko, I V Anoshkin, O N Efimov *Vysokomol. Soedin., Ser. B* **52** 724 (2010) [b]
304. P Yao, J Xu, Y Wang, C Zhu *J. Mater. Sci.: Mater. Electron.* **20** 891 (2009)
305. J Xu, P Yao, X Li, F He *Mater. Sci. Eng., B* **151** 210 (2008)
306. K-P Lee, A Y Gopalan, K S Kim, P Santhosh *J. Nanosci. Nanotechnol.* **7** 3386 (2007)
307. B Zhao, H Hu, A Yu, D Perea, R C Haddon *J. Am. Chem. Soc.* **127** 8197 (2005)
308. J Xu, P Yao, L Liu, Z Jiang, F He, M Li, J Zou *J. Appl. Polym. Sci.* **118** 2582 (2010)
309. S Yun, J Kim *Synth. Met.* **157** 523 (2007)

310. P Gomes-Romero *Adv. Mater.* **13** 163 (2001)
311. M G Kanatzidis, L M Tonge, T J Marks, H O Marcy, C R Kannewurf *J. Am. Chem. Soc.* **109** 3797 (1987)
312. M G Kanatzidis, C-G Wu, H O Marcy, D C DeGroot, C R Kannewurf, A Kostikas, V Papaefthymiou *Adv. Mater.* **2** 364 (1990)
313. M G Kanatzidis, M Hubbard, L M Tonge, T J Marks, H O Marcy, C R Kannewurf *Synth. Met.* **28** 89 (1989)
314. M G Kanatzidis, H O Marcy, W J McCarthy, C R Kannewurf, T J Marks *Solid State Ionics* **32 – 33** 594 (1989)
315. C-G Wu, H O Marcy, D C DeGroot, J L Schindler, C R Kannewurf, W-Y Leung, M Benz, E LeGoff, M G Kanatzidis *Synth. Met.* **41** 797 (1991)
316. C-G Wu, D C DeGroot, H O Marcy, J L Schindler, C R Kannewurf, T Bakas, V Papaefthymiou, W Hirpo, J P Yesinowski, Y-J Liu, M G Kanatzidis *J. Am. Chem. Soc.* **117** 9229 (1995)
317. A D Pomogailo, A S Rozenberg, I E Uflyand *Nanochastitsy Metallov v Polimerakh* (Nanoparticles of Metals in Polymers) (Moscow: Khimiya, 2000)
318. A De Stefanis, S Foglia, A A G Tomlinson *J. Mater. Chem.* **5** 475 (1995)
319. M G Kanaitzidis, C G Wu, H O Marcy, C R Kannewurf *J. Am. Chem. Soc.* **111** 4139 (1989)
320. C G Wu, D C DeGroot, H O Marcy, J L Schindler, C R Kannewurf, Y J Liu, W Hirpo, M G Kanatzidis *Chem. Mater.* **8** 1992 (1996)
321. V Petkov, V Parvanov, P Trikalitis, C Malliakas, T Vogt, M G Kanatzidis *J. Am. Chem. Soc.* **127** 8805 (2005)
322. F Huguenin, R M Torresi *J. Phys. Chem. C* **112** 2202 (2008)
323. S Pang, G Li, Z Zhang *Macromol. Rapid Commun.* **26** 1262 (2005)
324. M Malta, L H Silva, A Galembeck, M Korn *Macromol. Rapid Commun.* **29** 1221 (2008)
325. G Li, S Pang, L Jiang, Z Guo, Z Zhang *J. Phys. Chem. B* **110** 9383 (2006)
326. G Li, K Chao, C Zhang, Q Zhang, H Peng, K Chen *Inorg. Chem.* **48** 1168 (2009)
327. C Zhang, L Wang, H Peng, K Chen, G Li *Polym. Int.* **58** 1422 (2009)
328. J Dexmer, C M Leroy, L Binet, V Heresanu, P Launois, N Steunou, C Coulon, J Maquet, N Brun, J Livage, R Backov *Chem. Mater.* **20** 5541 (2008)
329. V D Pokhodenko, V A Krylov, Ya I Kurys, O Yu Posudievsky *Phys. Chem. Chem. Phys.* **1** 905 (1999)
330. B-Z Lin, C Diang, B-H Xu, Z-J Chen, Y-L Chen *Mater. Res. Bull.* **44** 719 (2009)
331. R Bissessur, W White *Mater. Chem. Phys.* **99** 214 (2006)
332. M G Kanatzidis, R Bissessur, D C DeGroot, J L Schindler, C R Kannewurf *Chem. Mater.* **5** 595 (1993)
333. R Bissessur, D Gallant, R Brüning *Mater. Chem. Phys.* **82** 316 (2003)
334. R Bissessur, P K Y Liu *Solid State Ionics* **177** 191 (2006)
335. M A Ibrahim, B-G Lee, N-G Park, J R Pugh, D D Ebert, A J Frank *Synth. Met.* **105** 35 (1999)
336. R Bissessur, W White, D C Dahn *Mater. Lett.* **60** 248 (2006)
337. L Wang, J Schindler, J A Thomas, C R Kannewurf, M G Kanatzidis *Chem. Mater.* **7** 1753 (1995)
338. B-Z Lin, X-K Pei, J-F Zhang, G-H Han, Z Li, P-D Liu, J-H Wu *J. Mater. Chem.* **14** 2001 (2004)
339. T Wang, W Liu, J Tian, X Shao, D Sun *Polym. Compos.* **25** 111 (2004)
340. A H Reshak, S Auluck *Phys. Rev. B: Condens. Matter* **68** 125101 (2003)
341. A H Reshak, S Auluck *Phys. Rev. B: Condens. Matter* **71** 155114 (2005)
342. R Bissessur, R I Haines, R Brüning *J. Mater. Chem.* **13** 44 (2003)
343. E Ruiz-Hitzky *Adv. Mater.* **5** 334 (1993)
344. *Polymer-Clay Nanocomposites* (Eds T J Pinnavaia, G W Beall) (Chichester: Wiley, 2000)
345. N Ballav, M Biswas *Synth. Met.* **142** 309 (2004)
346. Q H Zeng, A B Yu, G Q (Max) Lu, D R Paul *J. Nanosci. Nanotechnol.* **5** 1574 (2005)
347. J D Sudha, T S Sasikala *Polymer* **48** 338 (2007)
348. R M G Rajapakse, R M M Y Rajapakse, H M N Bandara, B S B Karunarathne *Electrochim. Acta* **53** 2946 (2008)
349. M R Karim, J H Yeum *J. Polym. Sci., Part B: Polym. Phys.* **46** 2279 (2008)
350. J W Kim, F Liu, H J Choi, S H Hong, J Joo *Polymer* **44** 289 (2003)
351. N Toshima, S Hara *Prog. Polym. Sci.* **20** 155 (1995)
352. H Inoue, H Yoneyama *J. Electroanal. Chem.* **233** 291 (1987)
353. S Yoshimoto, F Ohashi, Y Ohnishi, T Nonami *Synth. Met.* **145** 265 (2004)
354. A Shakoor, T Z Rizvi, A N Sangra *Vysokomol. Soedin., Ser. A* **52** 1780 (2010) [b]
355. A V Semakov, A A Shabeko, S G Kiseleva, A V Orlov, A V Rebrov, Yu M Korolev, G P Karpacheva, V N Kuleznev, V G Kulichikhin *Vysokomol. Soedin., Ser. B* **52** 341 (2010) [b]
356. G P Karpacheva, A V Orlov, S G Kiseleva, S Zh Ozkan, O Yu Yurchenko, G N Bondarenko *Elektrokhimiya* **40** 346 (2004) [j]
357. A V Orlov, S G Kiseleva, G P Karpacheva *Vysokomol. Soedin., Ser. A* **50** 1749 (2008) [b]
358. S Xing, C Zhao, S Jing, Z Wang *J. Mater. Sci.* **41** 2761 (2006)
359. D Lee, K Char, S W Lee, Y W Park *J. Mater. Chem.* **13** 2942 (2003)
360. H L Frisch, B Xi, Y Qin, M Rafailovich, N-L Yang, X Yan *High Perform. Polym.* **12** 543 (2000)
361. D Lee, K Char *Polym. Degrad. Stab.* **75** 555 (2002)
362. L Dai, Q Wang, M Wan *J. Mater. Sci. Lett.* **19** 1645 (2000)
363. R M G Rajapakse, D T B Tennakoon, J S H Q Perera, W M A T Bandara, D M M Krishantha *J. Compos. Mater.* **39** 1985 (2005)
364. W J Bae, K H Kim, W H Jo, Y H Park *Macromolecules* **37** 9850 (2004)
365. N Ballav, P Saha Sardar, S Ghosh, M Bismas *J. Mater. Sci.* **41** 2959 (2006)
366. V Mehrotra, E P Giannelis *Solid State Commun.* **77** 155 (1991)
367. V Mehrotra, E P Giannelis *Solid State Ionics* **51** 115 (1992)
368. K Ramachandran, M M Lerner *J. Electrochem. Soc.* **144** 3739 (1997)
369. K S Novoselov, A K Geim, S V Morozov, D Jiang, M I Katsnelson, I V Grigorieva, S V Dubonos, A A Firsov *Nature (London)* **438** 197 (2005)
370. Y Zhang, Y-W Tan, H L Stormer, P Kim *Nature (London)* **438** 201 (2005)
371. J C Meyer, A K Geim, M I Katsnelson, K S Novoselov, T J Booth, S Roth *Nature (London)* **446** 60 (2007)
372. S P Gubin, S V Tkachev *Grafen i Rodstvennye Formy Ugleroda* (Graphene and Related Forms of Carbon) (Moscow: Librokom, 2012)
373. N A Kotov, I Dékány, J H Fendler *Adv. Mater.* **8** 637 (1996)
374. H Bai, Y Xu, L Zhao, C Li, G Shi *Chem. Commun.* 1667 (2009)
375. Q Wu, Y Xu, Z Yao, A Liu, G Shi *ACS Nano* **4** 1963 (2010)
376. H Wang, Q Hao, X Jang, L Lu, X Wang *ACS Appl. Mater. Interfaces* **2** 821 (2010)
377. X Zhou, T Wu, G Yang, B Han *Chem. Commun.* **46** 3663 (2010)
378. L Q Xu, Y L Liu, K-G Neoh, E-T Kang, G D Fu *Macromol. Rapid Commun.* **32** 684 (2011)
379. D Li, M B Mmller, S Gilje, R B Kaner, G G Wallace *Nat. Nanotechnol.* **3** 101 (2008)

380. J Zhang, H Yang, G Shen, P Cheng, J Zhang, S Guo *Chem. Commun.* **46** 1112 (2010)
381. Z Mo, H Shi, H Chen, G Niu, Z Zhao, Y Wu *J. Appl. Polym. Sci.* **112** 573 (2009)
382. P Liu, K Gong, P Xiao, M Xiao *J. Mater. Chem.* **10** 933 (2000)
383. G Chen, C Wu, W Weng, D Wu, W Yan *Polymer* **44** 1781 (2003)
384. L Nikzad, S Alibeigi, M R Vaezi, B Yazdani, M R Rahimipour *Chem. Eng. Technol.* **32** 861 (2009)
385. G Chen, D Wu, W Weng, C Wu *Carbon* **41** 619 (2003)
386. G Gheno, N R de Souza Basso, R Hübler *Macromol. Symp.* **299 – 300** 74 (2011)
387. C Y Wang, V Mottaghitalab, C O Too, G M Spinks, G G Wallace *J. Power Sources* **163** 1105 (2007)
388. X Yan, J Chen, J Yang, Q Xue, P Miele *ACS Appl. Mater. Interfaces* **2** 2521 (2010)
389. W P Halperin *Rev. Mod. Phys.* **58** 533 (1986)
390. A P Alivisatos *Science* **271** 933 (1996)
391. A P Alivisatos *J. Phys. Chem.* **100** 13226 (1996)
392. L Brus *Appl. Phys. A: Mater. Sci. Process.* **53** 465 (1991)
393. A Henglein *Chem. Rev.* **89** 1861 (1989)
394. A Hagfeldt, M Grätzel *Chem. Rev.* **95** 49 (1995)
395. B J Kim, J J Chiu, G-R Yi, D J Pine, E J Kramer *Adv. Mater.* **17** 2618 (2005)
396. P Poulin *Curr. Opin. Colloid Interface Sci.* **4** 66 (1999)
397. L Ramos, P Fabre, R Ober *Eur. Phys. J. B* **1** 319 (1998)
398. P Poulin, H Stark, T C Lubensky, D A Weitz *Science* **275** 1770 (1997)
399. D Spoliansky, V Ponsinet, J Ferré, J-P Jamet *Eur. Phys. J. E* **1** 227 (2000)
400. L Ramos, P Fabre, L Fruchter *Eur. Phys. J. B* **8** 67 (1999)
401. N Kanayama, O Tsutsumi, A Kanazawa, T Ikeda *Chem. Commun.* 2640 (2001)
402. M Mitov, C Portet, Ch Bourgerette, E Snoeck, M Verelst *Nat. Mater.* **1** 229 (2002)
403. J Hu, L-s Li, W Yang, L Manna, L-w Wang, A P Alivisatos *Science* **292** 2060 (2001)
404. J Mmller, C Slnnichsen, H von Poschinger, H von Plessen, T A Klar, J Feldmann *Appl. Phys. Lett.* **81** 171 (2002)
405. H Duran, B Gazdecki, A Yamashita, T Kyu *Liq. Cryst.* **32** 815 (2005)
406. S Khatua, P Manna, W -S Chang, A Tcherniak, E Fiedlander, E R Zubarev, S Link *J. Phys. Chem. C* **114** 7251 (2010)
407. F Haraguchi, K-i Inoue, N Toshima, S Kobayashi, K Takatoh *Jpn. J. Appl. Phys., Part 2* **46** L796 (2007)
408. Y Reznikov, O Buchnev, O Tereshchenko, V Reshetnyak, A Glushchenko, J West *Appl. Phys. Lett.* **82** 1917 (2003)
409. C P Lapointe, T G Mason, I I Smalyukh *Science* **326** 1083 (2009)
410. J Milette, S J Cowling, V Toader, C Lavigne, I M Saez, R B Lennox, J W Goodby, L Reven *Soft Matter* **8** 173 (2012)
411. J Mirzaei, M Urbanski, K Yu, H-S Kitzerow, T Hegmann *J. Mater. Chem.* **21** 12710 (2011)
412. K K Vardanyan, R D Walton, D M Bubb *Liq. Cryst.* **38** 1279 (2011)
413. B Kinkead, T Hegmann *J. Mater. Chem.* **20** 448 (2010)
414. R Pratibha, W Park, I I Smalyukh *J. Appl. Phys* **107** 063511 (2010)
415. Q Liu, Y Cui, D Gardner, X Li, S He, I I Smalyukh *Nano Lett.* **10** 1347 (2010)
416. R Bitar, G Agez, M Mitov *Soft Matter* **7** 8198 (2011)
417. D E Fogg, L H Radzilowski, R Blanski, R R Schrock, E L Thomas *Macromolecules* **30** 417 (1997)
418. W A Lopes, H M Jaeger *Nature (London)* **414** 735 (2001)
419. W A Lopes *Phys. Rev. E* **65** 031606 (2002)
420. M J Misner, H Skaff, T Emrick, T P Russell *Adv. Mater.* **15** 221 (2003)
421. T Thurn-Albrecht, R Steiner, J DeRouchey, C M Stafford, E Huang , M Bal, M Tuominen, C J Hawker, T P Russell *Adv. Mater.* **12** 787 (2000)
422. A Böker, J He, T Emrick, T P Russell *Soft Matter* **3** 1231 (2007)
423. Q Li, J He, E Glogowski, X Li, J Wang, T Emrick, T P Russell *Adv. Mater.* **20** 1462 (2008)
424. Q Zhang, S Gupta, T Emrick, T P Russell *J. Am. Chem. Soc* **128** 3898 (2006)
425. Y Lin, A Böcker, J He, K Sill, H Xiang, C Abetz, X Li, J Wang, T Emrick, S Long, Q Wang, A Balazs, T P Russell *Nature (London)* **434** 55 (2005)
426. Y -H Ha, Y Kwon, T Breiner, E P Chan, T Tzianetopoulou, R E Cohen, M C Boyce, E L Thomas *Macromolecules* **38** 5170 (2005)
427. B J Kim, J Bang, C J E Hawker, E J Kramer *Macromolecules* **39** 4108 (2006)
428. H Yabu, T Jinno, K Koike, T Higuchi, M Shimomura *Macromolecules* **44** 5868 (2011)
429. R B Thompson, V V Ginzburg, M W Matsen, A C Balazs *Macromolecules* **35** 1060 (2002)
430. S Gupta, Q Zhang, T Emrick, A C Balazs, T P Russell *Nat. Mater.* **5** 229 (2006)
431. S W Sides, B J Kim, E J Kramer, G H Fredrickson *Phys. Rev. Lett.* **96** 250601 (2006)
432. H Yabu, T Jinno, K Koike, T Higuchi, M Shimomura *J. Polym. Sci., Part B: Polym. Phys.* **49** 1717 (2011)
433. K Aissou, G Fleury, G Pecastaings, T Alnasser, S Mornet, G Goglio, G Hadziioannou *Langmuir* **27** 14481 (2011)
434. R Shenhar, T B Norsten, V M Rotello *Adv. Mater.* **17** 657 (2005)
435. R L Phillips, O R Miranda, D E Mortenson, C Subramani, V M Rotello, U H F Bunz *Soft Matter* **5** 607 (2009)
436. H Xu, R Hong, X Wang, R Arvizo, C You, B Samanta, D Patra, M T Tuominen, V M Rotello *Adv. Mater.* **19** 1383 (2007)
437. J Pérez-Juste, B Rodríguez-Gonzáles, P Mulvaney, L M Liz-Marzan *Adv. Funct. Mater.* **15** 1065 (2005)
438. S Meuer, P Oberle, P Theato, W Tremel, R Zentel *Adv. Mater.* **19** 2073 (2007)
439. M Zorn, S Meuer, M Nawaz Tahir, Y Khalavka, C Sönnichsen, W Tremel, R Zentel *J. Mater. Chem.* **18** 3050 (2008)
440. S Meuer, K Fischer, I Mey, A Janshoff, M Schmidt, R Zentel *Macromolecules* **41** 7946 (2008)
441. A S Merekalov, S A Kuptsov, G A Shandryuk, R V Talroze, V S Bezborodov, E M Terentjev *Liq. Cryst.* **28** 495 (2001)
442. A M Shatalova, G A Shandryuk, G N Bondarenko, S A Kuptsov, R V Tal'roze, N A Plate *Vysokomol. Soedin., Ser. A* **45** 245 (2003) [b]
443. R B Vasiliev, S G Dorofeev, D N Dirin, D A Belov, T A Kuznetsova *Mendeleev Commun.* 169 (2004)
444. G A Shandryuk, A V Rebrov, R B Vasil'ev, S G Dorofeev, A S Merekalov, A M Gas'kov, R V Tal'roze *Vysokomol. Soedin., Ser. B* **47** 1879 (2005) [b]
445. F Shieh, A E Saunders, B A Korgel *J. Phys. Chem. B* **109** 8538 (2005)
446. RF P. 2414491 (2011)
447. G Shandryuk, A Merekalov, V Bykov, G Bondarenko, R Vasiliev, A Gaskov, R Talroze *Polym. Prepr.* **48** 795 (2007)
448. A A Ezhov, G A Shandryuk, G N Bondarenko, A S Merekalov, S S Abramchuk, A M Shatalova, P Manna, E R Zubarev, R V Talroze *Langmuir* **27** 13353 (2011)
449. G A Shandryuk, E V Matukhina, R B Vasil'ev, A Rebrov, G N Bondarenko, A S Merekalov, A M Gas'kov, R V Talroze *Macromolecules* **41** 2178 (2008)

450. R V Tal'roze, G A Shandryuk, A S Merekalov, A M Shatalova, O A Otmakhova *Vysokomol. Soedin., Ser. A* **51** 1930 (2009) [b]
451. A G Joly, W Chen, D E McCready, J-O Malm, J-O Bovin *Phys. Rev. B: Condens. Matter* **71** 165304 (2005)
452. F A J M Driessen *Appl. Phys. Lett.* **67** 2813 (1995)
453. Yu P Rakovich, S A Filonovich, M J M Gomes, J F Donegan, D V Talapin, A L Rogach, A Eychmüller *Phys. Status Solidi B* **229** 449 (2002)

[a] — *Dokl. Phys. Chem. (Engl. Transl.)*
[b] — *Polym. Sci. (Engl. Transl.)*
[c] — *J. Eng. Phys. Thermophys. (Engl. Transl.)*
[d] — *Colloid. J. (Engl. Transl.)*
[e] — *Nanotechnol. Russ. (Engl. Transl.)*
[f] — *Phys. Solid State (Engl. Transl.)*
[g] — *Russ. J. Appl. Chem. (Engl. Transl.)*
[h] — *Mendeleev Chem. J. (Engl. Transl.)*
[i] — *J. Superhard Mater. (Engl. Transl.)*
[j] — *Russ. J. Electrochem. (Engl. Transl.)*